



Application of pulsed electric fields for the biocompatible extraction of proteins from the microalga *Haematococcus pluvialis*

Hélène Gateau, Vincent Blanckaert, Brigitte Veidl, Odile Burlet-Schultz, Carole Pichereaux, Audrey Gargaros, Justine Marchand, Benoît Schoefs

► To cite this version:

Hélène Gateau, Vincent Blanckaert, Brigitte Veidl, Odile Burlet-Schultz, Carole Pichereaux, et al.. Application of pulsed electric fields for the biocompatible extraction of proteins from the microalga *Haematococcus pluvialis*. *Bioelectrochemistry*, 2021, 137, pp.107588. <10.1016/j.bioelechem.2020.107588>. <hal-03493886>

HAL Id: hal-03493886

<https://hal.science/hal-03493886v1>

Submitted on 7 Nov 2022

HAL is a multi-disciplinary open access archive for the deposit and dissemination of scientific research documents, whether they are published or not. The documents may come from teaching and research institutions in France or abroad, or from public or private research centers.

L'archive ouverte pluridisciplinaire **HAL**, est destinée au dépôt et à la diffusion de documents scientifiques de niveau recherche, publiés ou non, émanant des établissements d'enseignement et de recherche français ou étrangers, des laboratoires publics ou privés.



Distributed under a Creative Commons CC BY-NC 4.0 - Attribution - Non-commercial use - International License

Application of pulsed electric fields for the biocompatible extraction of proteins from the microalga *Haematococcus pluvialis*¹

Hélène GATEAU¹, Vincent BLANCKAERT², Brigitte VEIDL¹, Odile BURLET-SCHILTZ³, Carole PICHEREAUX^{3,4}, Audrey GARGAROS⁵, Justine MARCHAND^{1,6} & Benoît SCHOEFS^{1,6,*}

¹ Metabolism, Bioengineering of Molecules from Microalgae and Applications (MIMMA), Mer Molécules Santé, IUML – FR 3473 CNRS, Le Mans University, Le Mans, France

² Metabolism, Bioengineering of Molecules from Microalgae and Applications (MIMMA), Mer Molécules Santé, IUML – FR 3473 CNRS, IUT de Laval, Le Mans University, Le Mans, France

³ Institut de Pharmacologie et de Biologie Structurale (IPBS), Université de Toulouse UPS, CNRS, Toulouse, France

⁴ Fédération de Recherche (FR3450), Agrobiosciences, Interactions et Biodiversité (FRAIB), CNRS, Toulouse, France

⁵ Evotec SAS, 195 Route d'Espagne – BP13669, Toulouse, France

6 : JM and BS share the senior authorship

* Corresponding author. Benoît Schoefs. Address: MIMMA, Le Mans University, Mer Molécules Santé (MMS), Avenue O. Messiaen, 72000 Le Mans, France. E-mail address: Benoit.Schoefs@univ-lemans.fr

ABSTRACT

This study aims to employ a pulsed electric field (PEF) treatment for the biocompatible (non-destructive) extraction of proteins from living cells of the green microalga *Haematococcus pluvialis*. Using a field strength of 1 kV cm⁻¹, we achieved the extraction of 10.2 µg protein per mL of culture, which corresponded to 46% of the total amount of proteins that could be extracted by complete destructive extraction (i.e. the

¹ACP: acyl carrier protein, ADK: adenylate kinase, A_{XXX}: absorbance at XXX nm, BI: biocompatibility index, CBB: Calvin-Benson-Bassham, CF: coupling factor, EF-1α: eukaryotic translation elongation factor 1 alpha, ER: endoplasmic reticulum, FA: fatty acid, FNR: ferredoxin:NADP⁺ reductase, GP: gross photosynthesis, HSP: heat-shock protein, IP: irreversibly permeabilized, LSU: large subunit, N-PEF: naturally permeabilized without PEF treatment but with cell processing, NA: nonaffected, NAT-P: naturally permeabilized without PEF treatment and without cell processing, NP: net photosynthesis, p: permeabilized, PBR: photobioreactor, PCR: polymerase chain reaction, PEF: pulsed electric fields, pp: potentially permeabilized, PS: photosystem, R: respiration, ROS: reactive oxygen species, RP: reversibly permeabilized, RuBisCO: ribulose-1,5-bisphosphate carboxylase oxygenase, RuBP: ribulose-1,5-bisphosphate, SAM: S-adenosylmethionine, SOD: superoxide dismutase, TAG: triacylglycerol

grinding of biomass with glass beads). We found that the extraction yield was not improved by stronger field strengths and was not dependent on the pulse frequency. A biocompatibility index (BI) was defined as the relative abundance of cells that remained alive after the PEF treatment. This index relied on measurements of several physiological parameters after a PEF treatment. This way found that at 1 kV cm^{-1} that cultures recovered after 72 h. Therefore, these PEF conditions constituted a good compromise between protein extraction efficiency and culture survival. To characterize the PEF treatment further at a molecular level, mass spectrometry-based proteomics analyses of PEF-prepared extracts was used. This led to the identification of 52 electro-extracted proteins. Of these, only 16 proteins were identified when proteins were extracted with PEF at 0.5 cm^{-1} . They belong to core metabolism, stress response and cell movement. Unassigned proteins were also extracted. Their physiological implications and possible utilization in food as alimentary complements are discussed.

KEYWORDS

pulsed electric field, biocompatibility, protein electroextraction, reversible permeabilization, biotechnology

1. INTRODUCTION

The increase of human populations and the expansion of cities contribute to an accelerated depletion of agricultural lands and natural resources. To overcome this challenge, an intensive search for alternative sources of biological molecules has started. Proteins are a cornerstone of health and wellness, accounting for half of the market for nutritional and functional ingredients [1]. The protein market size continues to increase, mostly because of the belief that proteins from traditional sources, i.e. meat, may trigger inflammation [1]. Moreover, a diet containing non-animal sourced proteins is beneficial because they are rich in essential amino acids, such as cysteine, which is used by the body to replenish skin cells and support hair growth. Microalgae are a promising source for the production of these biomolecules because they are ubiquitous microorganisms that are known to produce a high variety of molecules including proteins, while utilizing sun energy through the process of photosynthesis [2]. Microalgae constitute an interesting alternative source for protein production because proteins can represent up to 65% of their weight [3]. In addition, through genetic engineering and synthetic biology, microalgae might be used as a very efficient platform for the nontransgenic and transgenic production of proteins that accumulate inside the cells. However, because microalgal cells are often surrounded by a rigid cell wall, the extraction of internal compounds requires a complete cell disintegration. Thus, regardless of the desired final product, microalgal biotechnological processes start with the cultivation of the algae to obtain a substantial biomass, after which this biomass is harvested and processed according to a specific downstream procedure. A recent analysis pointed out three main disadvantages of current downstream processes: (1) the unselective extraction of cellular compounds which results in the need for additional purification steps, (2) the generation of biological and organic wastes because of the use

of solvents, and (3) the energy and time required for the processing [4]. To reduce these drawbacks, it is thus clear that alternative, eco-friendly processes have to be developed.

Since the pioneering work on membrane electroporation, pulsed electric fields (PEFs) have been used in many biotechnological applications (for a review, see [5]). PEFs have also been considered as an efficient tool for the downstream biotechnological processing of biomass [5]. For example, it has been used for the electro-extraction of water-soluble proteins from microalgae such as *Chlorella vulgaris*, *Haematococcus pluvialis*, and *Nannochloropsis salina* [6]. Used as a pre-treatment prior to solvent extraction, PEF treatment improved the extraction yield of microalgal compounds, thus allowing a reduction in the volume of the used solvent (for a review, see [7]). Furthermore, this process is more energy-efficient because no drying step is necessary compared to classical processing methods which require the dewatering, drying, grinding, extraction of biomass followed by the purification of the extracted compounds [7].

Besides these studies, where PEF treatments have been tested for their extraction capacity, the impact of PEF treatments on microalgae physiology has not been well investigated. Such insights, however, are required to understand how PEF treatments impact the viability of the cells, and to develop a biocompatible PEF-based extraction process that leaves the cells in a viable state. This knowledge is needed for the application of milking protocols i.e. repetitive treatment to microalgae. It is known that PEFs trigger pore formation in the plasmalemma through which molecules are exchanged [5]. Furthermore, the field intensity, as well as the pulse frequency and the pulse duration, impact cell viability [5]. As a result, the PEF treatment of a microalgal population leaves each cell in one of the 3 following states: (1) dead cells that have lost their plasmalemma integrity and in which metabolic activity is absent, (2) non-permeabilized viable cells that have an intact plasmalemma and an active metabolism, (3) injured cells that experienced a transient loss of plasmalemma integrity but which have preserved a functional metabolism. It is thought that the capacity of the plasmalemma to reseal determines in which of these states a given cell will reside, and thus it eventually determines the biocompatibility of the PEF treatment. According to Bodénès, Bensalem, Français, Pareau, Le Pioufle and Lopes [8] membrane resealing should occur within 30 s following the electric pulse in order for the cell to remain viable. When the parameters of the PEF treatment are adequately adjusted, this kind of treatment indeed allows to reversibly increase the permeability of the plasma membrane, thus facilitating the exchange of compounds from the inside of cells to the outside, and *vice versa*, without killing the cells [9]. It is thus clear that the use of a biocompatible PEF treatment has a real potential for the recovery of microalgal biomolecules during downstream processing.

In this study, PEF conditions are reported that allow a biocompatible electroextraction of water-soluble proteins from a new strain of the freshwater green alga *H. pluvialis* (Flotow) (Chlamydomonadales). The cell cycle of *H. pluvialis* is dominated by three stages: red cysts characterized by a high astaxanthin content and a thick cell wall, green macrozooids, and palmellas. Macrozooids are motile and pear-shaped cells whereas palmellas are non motile and spherical [10]. The interest for the production of proteins from *Haematococcus* does not only stem from its nutritional value (around 26% of proteins on dry weight basis), but also from its emulsifying properties [11]. Coustets,

Joubert-Durigneux, Hérault, Schoefs, Blanckaert, Garnier and Teissié [6] have shown the feasibility of electro-extracting water-soluble proteins from this green microalga, but without demonstrating the potential use of PEF treatments as a biocompatible extraction process. Electro-extracted proteins have been identified by proteomics based on mass spectrometry allowing the determination of the subcellular origin of electro-extracted proteins and the impact of their electro-extraction on the physiology of microalgae..

2. MATERIALS & METHODS

2.1. Strain identification, culture conditions and sample preparation

Samples of *H. pluvialis* were collected in Tournlaville (49°39'20.60" N, 1°34'7.62" O), France. An axenic strain was prepared and identified using morphological criteria [12] and its taxonomic positioning was confirmed using 18S rRNA gene sequencing. The genomic DNA of the microalga was extracted according to the protocol of Doyle and Doyle [13] and treated by RNase. The 18S rRNA gene sequence was then amplified as two overlapping fragments by polymerase chain reaction (PCR) using the primers described in [14]. The PCR products were purified using the Wizard® SV Gel and PCR Clean-Up System kit (Promega, Madison, WI, USA), cloned into pGEM®-T vector (Promega, Madison, WI, USA) following the manufacturer's instructions and then sequenced by Beckman Coulter Genomics (Bishop's Stortford, UK). The two partial nucleotide sequences obtained were assembled to reconstruct the complete 18S rRNA gene sequence that was then compared to the NCBI database using BLASTn. In order to create a dataset of 18S rRNA nucleotide sequences of organisms belonging to the same clade than *H. pluvialis* (Chlamydomonadales), 37 sequences were imported from GeneBank and all aligned using Clustal 2.1. The multiple alignment was subsequently used to perform a phylogenetic analysis. The best evolutionary model (GTR) for the dataset was determined using PhyML 3.0 (<http://www.atgc-montpellier.fr>) and the phylogenetic analysis carried out using the maximum parsimony method. Nodal support of the tree was evaluated by a bootstrap analysis with 1,000 replicates. The new 18S rRNA sequence has been deposited in GenBank under the accession number LT578169.

To determine the primary nutritional group to which the new strain of *H. pluvialis* belongs, microalgae were grown in 250 mL Erlenmeyer flasks at 19°C with three different carbon sources: NaHCO₃ for MLA medium [15], Na₂CO₃ for BG11 medium [16] and acetate for TAP medium [17]. Unless otherwise stated, cultures were grown under a photon flux density of 35 µmol photons m⁻² s⁻¹ with a photoperiod of 14 h. Cell density was followed during 10 days: every day, 1 mL of the algal suspension was fixed with a Lugol's solution, then an aliquot of this preparation was transferred to a Malassez haemocytometer. The growth rate was calculated by fitting a logistic model to the experimental values of cell density using CurveExpert Basic 1.4 (<https://www.curveexpert.net/>). Culture conditions allowing the highest cell density were retained for the electroextraction experimentations. Before being treated by PEF, cells were collected after 8 days of growth and harvested by centrifugation (400 x g, 5 min, 19°C) (Fig. 1).

Here Schematic 1

The cell diameter (Féret diameter) after PEF treatment was determined using ImageJ ([http:// imagej.nih.gov/ij/](http://imagej.nih.gov/ij/)) analysis of pictures of 15 bright field images per replicate representing around 5000 cells. Pictures were taken using a Zeiss LSM 800 microscope using the Zen2 software (Zeiss) calibrated with a scalebar.

To avoid a temperature increase of the medium higher than 10°C during the PEF treatment, the pellet was resuspended in distilled water in order to attain a medium conductivity of about 20 $\mu\text{S cm}^{-1}$ (at the reference temperature of 25°C). This conductivity is required to avoid possible damage to both the equipment and the microalgae [18]. The microalgal suspension was diluted to a final cell concentration of 10^5 cells mL^{-1} .

2.2. Protein electroextraction

2.2.1. Experimental set-up

The electroextraction system was previously described in [19]. Briefly, the PEF treatment was carried out through two connected pulse generators (DEEX-Bio, β tech, Toulouse, France) allowing the delivery of pairs of bipolar square pulses within an electroporation chamber (CNRS, Toulouse, France). Two different chambers differing in the distance between the two plates electrodes (3 or 6 mm) have been used, thus allowing the application of two different maximal field strengths (6 or 3 kV cm^{-1} , respectively). The microalgae suspension flowed through the electroporation chamber thanks to a peristaltic pump (Fisher Scientific™ Variable-Flow Peristaltic Pump, Fisher Scientific, Pittsburgh, USA) and was submitted to a series of pulses. The flow rate (Q , mL s^{-1}) was calculated according to equation 1:

$$Q = (F * V) / N \quad (1)$$

where F is the repetition frequency of the pairs of pulses ($F = 9.62$ Hz), V the volume of the chamber (0.27 or 0.54 mL, respectively) and N the mean number of pairs of pulses applied on each cell in the electroporation chamber.

For each selected value of N (5 or 9 pairs of pulses), 6 different field strengths have been tested (0, 0.5, 1, 2, 3 or 6 kV cm^{-1}). For the 0 kV cm^{-1} field strength, chosen as a control condition, microalgae flowed through the electroporation chamber without pulse delivery. For the other strengths, electrical pulses were applied. The pulse duration was kept constant at 2 ms. The temperature and the conductivity of the microalgal suspensions were measured just before and immediately after the PEF treatment using a probe thermometer and a conductometer, respectively.

Unless otherwise stated, PEF-treated cell suspensions were incubated 45 min at room temperature to leave time for intracellular compounds to diffuse out of cells. In this manuscript, we will refer to this period as the post-treatment incubation period (Fig. 1). After this step, the suspensions were centrifuged ($400 \times g$, 5 min, 19°C) and the supernatants collected for protein and pigment quantifications. The pellets were resuspended in distilled water or in the growth medium (5.10^4 cells mL^{-1}) before

returning to the culture room to allow cells to recover from the PEF treatment. In this manuscript we will refer to this period as the recovery period (Fig. 1). During the recovery period, samples have been regularly harvested and analyzed.

2.2.2. Preparation of the negative and positive protein controls

Negative control

A sample of 2 mL of the microalgal suspension (10^5 cells mL⁻¹) in distilled water was centrifuged (400 x g, 5 min, 19°C) (Fig. 1). The cell pellet was resuspended in 2 mL of fresh distilled water and incubated for 45 min at room temperature. The suspension was then centrifuged (400 x g, 5 min, 19°C). The supernatant was immediately gathered and stored at - 20°C for protein quantification.

Positive control

A sample of 2 mL of the microalgae suspension (10^5 cells mL⁻¹) in distilled water was centrifuged (400 x g, 5 min, 19°C) (Fig. 1). The cell pellet was resuspended in the same volume of 70 mM phosphate buffer containing 0.09 M glycerol and 1 mM DTT and then 500 µL of glass beads (200-300 µm in diameter) were added to this suspension. The mixture was vortexed at maximum speed 8 times for 1 min each time. The suspension was maintained on ice for 15 s between each vortex cycle to avoid excessive heating. The sample was then stored at 4°C for 30 min before being centrifuged (400 x g, 5 min, 19°C). The supernatant was collected and stored at - 20°C for protein quantification.

2.2.3. Estimation of the permeability

Cell permeabilization was assayed using Evans blue dye. One mL of PEF-treated microalgal suspension was centrifuged (400 x g, 5 min, 19°C) and the supernatant was discarded. The cell pellet was incubated at room temperature with 500 µL of 0.2 % Evans blue solution for 15 min. The relative abundance of blue cells was calculated as the number of counted blue cells out of the total number of microalgae present in the counting chamber. The counting was performed 5 min or 45 min after the PEF treatment. The permeability was also measured for the negative control. In agreement with Bodénès, Bensalem, Français, Pareau, Le Pioufle and Lopes [8], four categories of cells can be distinguished: (1) the irreversibly permeabilized cells (IP), (2) the reversibly permeabilized cells (RP), (3) the non-affected cells (NA) and (4) the naturally permeabilized cells (NAT-P). Unlike in Bodénès, Bensalem, Français, Pareau, Le Pioufle and Lopes [8] who delivered the PEF inside a cuvette without cell processing, microalgae were brought to the PEF chambers using a peristaltic pump. Therefore, the impact of this manipulation on the cells was also estimated and the non-PEF naturally permeabilized category (N-PEF) was defined as the proportion of cells of the negative control that loaded Evans blue dye. Thus, after a PEF treatment, a sample contained a

certain proportion of each cell category. In addition, each cell could exist under two states: potentially permeabilized (pp) or permeabilized (p). Therefore we can write

$$100 = \text{N-PEF}_p (\%) + \text{IP}_{pp} (\%) + \text{RP}_{pp} (\%) + \text{NA}_{pp} (\%) \quad (2)$$

In the absence of PEF all cells remain by definition ‘potentially permeabilized’ but only NAT-P and N-PEF_p cells will be stained by Blue Evans. The other cell categories i.e. IP_{pp} (%), RP_{pp} (%) and NA_{pp} (%) cannot be distinguished individually but can be grouped and defined as the unstained cells (%) (Equation 3)

$$\text{Non-colored} (\%) = \text{IP}_{pp} (\%) + \text{RP}_{pp} (\%) + \text{NA}_{pp} (\%) \quad (3)$$

Thus, equation 2 can be rewritten as

$$\text{N-PEF}_p (\%) = 100 - (\text{Non-colored} (\%)) \quad (4)$$

where N-PEF_p is considered as constant provided that the same experimental protocol is used.

During the PEF treatment, cells may turn from pp status to p status resulting in the formation of IP_p, RP_p categories. Cells that have stayed in the pp status form the NA_{pp} category. After a PEF treatment, only IP_p and RP_p and N-PEF_p cells should be stained with Blue Evans. Thus, Equation 2 can be rewritten as

$$\text{IP}_p (\%) + \text{RP}_p (\%) + \text{N-PEF}_p (\%) = 100 - \text{NA}_{pp} (\%) \quad (5)$$

Equation 5 can be rewritten as

$$\text{IP}_p (\%) + \text{RP}_p (\%) = 100 - \text{NA}_{pp} (\%) - \text{N-PEF}_p (\%) \quad (6)$$

If we hypothesize that the reduction in gross photosynthesis is only due to cells that died during the PEF treatment and during the incubation period, then one can write that the relative decrease in oxygen production due to the formation of IP cells is

$$\text{IP}_p (\text{O}_2) = [(\text{O}_{2,0} \text{ kV cm}^{-1} - \text{O}_{2,i} \text{ kV cm}^{-1}) / \text{O}_{2,0} \text{ kV cm}^{-1}] \quad (7)$$

where i equals to the field strength and IP_p(O₂) represents IP_p (%).

The introduction of the result of Eq. 7 into Eq. 6 allows the determination of RP_p (%).

By definition, NA_{pp} and RP_p cells are alive after the PEF treatment. Their values can be combined to define the biocompatibility index (BI) that can be calculated using Equation 8.

$$\text{BI} (\%) = \text{NA}_p (\%) + \text{RP}_p (\%) \quad (8)$$

2.2.4. Energy input

The energy input (W_{PEF} , kJ/kg) during the PEF treatment was calculated according equation 9

$$W_{\text{PEF}} = (E_{\text{PEF}}^2 \Delta t_{\text{pulse}} \sigma_{\text{medium}} N_{\text{pulse}}) / \rho_{\text{medium}} \quad (9)$$

where E_{PEF} (V m^{-1}), Δt_{pulse} (s), σ_{medium} (S m^{-1}), N_{pulse} and ρ_{medium} (kg m^{-3}) represent the electric field amplitude, the pulse duration, the medium conductivity, the number of pulses and the medium density, respectively.

2.4. Analysis of the electro-extracted microalgal components

2.4.1. Analysis of released pigments

The absorbance spectrum of the supernatant was recorded at room temperature in the range from 400 to 800 nm using a double beam UV/Vis spectrophotometer (LAMBDA™ 25, PerkinElmer, Beaconsfield, UK). The reference cuvette was filled with distilled water. The spectrum was then corrected for the absorbance at 800 nm. The determination of the wavelengths at which maximal absorbance occurred was based on the maxima of the 4th derivative of the corrected absorbance spectrum [20].

2.4.2. Water-soluble proteins quantification

The concentration of water-soluble proteins was determined using the Bradford assay (Bradford, 1976). Briefly, a sample of 800 μL of each supernatant was mixed with 200 μL of Bradford reagent (BioRad, Marnes la Coquette, France) by pipetting directly into a spectrophotometer cuvette. The mixture was incubated 5 min at room temperature before measuring its absorbance at 595 nm by a double beam UV/Vis spectrophotometer (LAMBDA™ 25, PerkinElmer, Beaconsfield, UK). The reference cuvette was filled with the Bradford reagent diluted in distilled water (1:5, v/v). Bovine serum albumin (Sigma, St Louis, USA) was used as protein standard for generating the calibration curve.

2.5. Determination of the physiological state of the treated cultures

2.5.1. Photosynthetic oxygen evolution and the maximum quantum yield of photosystem II photochemistry

Two samples of each PEF-treated microalgal suspension were collected and diluted to a final volume of 2 mL with TAP medium so that the chlorophyll (Chl) *a* amount was the same, i.e. $A_{678} - A_{800} = 0.04$, where A_{678} and A_{800} represent the absorbance at 678 nm and 800 nm, respectively. The temperature was kept constant at 19°C (growth temperature) during the whole measurement period.

To measure the photosynthetic oxygen evolution of the PEF-treated cells, the sample was placed into a double walled vial. The REDFLASH technology, combined with an oxygen meter (FireSting O₂, PyroScience, Aachen, Germany) connected to a computer, was used to carry out the measurements. Cells were first exposed to an actinic light of

35 μmol of photons $\text{m}^{-2} \text{s}^{-1}$ until the O_2 concentration measured inside the vial increased linearly for at least 3 min. The oxygen amount actually released during this period corresponds to the net photosynthesis (NP) ($\text{mg L}^{-1} \text{h}^{-1}$). Cells were then placed in the dark to measure the amount of O_2 consumed by respiration (R; $\text{mg L}^{-1} \text{h}^{-1}$). Gross photosynthesis (GP in $\text{mg O}_2 \text{h}^{-1} \text{mg Chl } a^{-1}$) of each sample was calculated according to Equation 10

$$\text{GP} = (\text{NP} + |\text{R}|) / [\text{Chl } a] \quad (10)$$

where $|\text{R}|$ is the absolute value of the respiration rate ($\text{mg L}^{-1} \text{h}^{-1}$) and $[\text{Chl } a]$ is the Chl a concentration in the sample (mg L^{-1}). This equation is based on the assumption that the respiration rate was the same in the light and in the dark.

The maximum quantum yield of photosystem II (PS II) photochemistry was determined following the protocol described in [21]. All measurements were recorded using a FMS1 pulse modulated chlorophyll fluorometer (Hansatech Instruments, King's Lynn, UK). The maximum variable fluorescence yield (F_v/F_m) was calculated according to Equation 11

$$F_v/F_m = (F_m - F_o)/F_m \quad (11)$$

The definition of the different Chl a fluorescence levels is summarized in [21].

2.5.2. Macrozooid motility

Cell motility is expressed as the percentage of motile cells divided by the total number of cells as determined through microscopic assessment using a Malassez haemocytometer.

2.6. Mass spectrometry-based proteomics analysis

2.6.1. Protein recovery

Proteins that were electro-extracted by PEF conditions at 0.5 ($P_{0.5}$) and 1 kV cm^{-1} ($P_{1.0}$) were prepared from a volume of 12 mL of PEF-treated cells. Their respective concentrations were 0.04 and 0.08 mg mL^{-1} , respectively. Proteins were precipitated with trichloroacetic acid (20:100 V/V) (Merck, Molsheim, France) during 24 h at 4°C followed by a filtration on a surface of 1.26 cm^2 using a Millipore filtration system equipped with Glass microfiber filters (Grade GF/F, Whatman®, GE Healthcare, Villebon-sur-Yvette, France). The filters were rinsed with ultrapure water, dried and placed in Eppendorf tubes. The proteins were solubilized with 150 μL of a Destreak® solution (GE Healthcare, Vélizy-Villacoublay, France). Samples were then prepared for electrophoresis by adding a sample buffer containing Tris/HCl 0.6M, pH 6.8 with 2% SDS, 40 mM DTT and 10% glycerol (ratio 33:17).

2.6.2. One-dimensional gel electrophoresis

Two hundred micrograms of proteins were loaded onto a 12 % polyacrylamide electrophoresis gel according to Laemmli [22]. The upper and lower chambers were

filled with a Tris-glycine buffer. The electrophoresis was conducted at 8 W until all the pre-stained molecular weight markers were distinguishable. After migration, the gels were washed twice for 5 min with ultrapure water to remove chemicals. The gel was incubated overnight at room temperature on a gel shaker with the Imperial Blue[®] dye (Thermo-Fisher, Villebon-sur-Yvette, France). Prior to scanning on a densitometer (GS800, Bio-Rad), the gel was destained with ultrapure water until the background in the gel became faint or invisible. .

2.6.3. MS/MS analysis of the proteins

Sample preparation

1-DE gel bands were excised, washed twice with 50 mM ammonium bicarbonate-acetonitrile (1:1, v:v) and then washed once with acetonitrile. Proteins were in-gel digested by the addition of 60 µL of a solution of modified sequencing-grade trypsin dissolved in 25 mM ammonium bicarbonate (20 ng/µL, sequence grade, Promega, Charbonnières, France). The mixture was incubated at 37 °C overnight. The resulting peptides were extracted from the gel by one round of incubation (15 min, 37°C) in 1% formic acid–acetonitrile (40%) and two rounds of incubation (15 min each, 37°C) in 1% formic acid–acetonitrile (1:1). The extracted fractions were air-dried. Tryptic peptides were resuspended in 14 µl of 2% acetonitrile and 0.05% trifluoroacetic acid for further MS analysis.

Nano-LC-MS/MS analysis

Peptide mixtures were analysed by nano-LC-MS/MS using a nanoRS UHPLC system (Dionex, Amsterdam, The Netherlands) coupled to a LTQ-Orbitrap Velos mass spectrometer (Thermo Fisher Scientific, Bremen, Germany). Five microliters of each sample were loaded on a C18 pre-column (5 mm × 300 µm; Dionex) at 20 µL/min in 2% acetonitrile, 0.05% trifluoroacetic acid. After 5 min of desalting, the pre-column was switched on line with the analytical C18 column (15 cm × 75 µm; in-house packed) equilibrated in 95% of mixture A (5% acetonitrile + 0.2% formic acid in water) and 5% of mixture B (80% acetonitrile + 0.2% formic acid in water). Peptides were eluted using a 5-50% gradient of B during 105 min at a 300 nL/min flow rate. The LTQ-Orbitrap was operated in data-dependent acquisition mode with the Xcalibur software. Survey scan MS spectra were acquired in the Orbitrap on the 300–2000 *m/z* range with the resolution set to a value of 60000. The twenty most intense ions per survey scan were selected for CID fragmentation, and the resulting fragments were analysed in the linear trap quadrupole (LTQ). Dynamic exclusion was used within 60 s to prevent repetitive selection of the same peptide.

Bioinformatics analysis of nano-LC-MS/MS data

The MS and MS/MS data files were converted to the mzdb format and processed with the mzdb-access library (<https://github.com/mzdb>) to generate peaklists. Data were searched with Mascot (version 2.6.1, <http://matrixscience.com>) against a custom-made database containing all *Chlamydomonas* + *Haematococcus pluvialis* entries from the UniProtKB database (Swiss-Prot/TrEmbl release 20160321, 16 780 235 entries). The search included methionine oxidation as a variable modification, and

carbamidomethylation of cysteine as a fixed modification. Specificity of digestion was set for cleavage after lysine or arginine for trypsin-digested samples, and one missed cleavage was allowed. The mass tolerance was set to 6 ppm for the precursor ion. It was set to 0.6 Da for fragment ions in CID mode (detection in the ion trap). Validation of identifications was performed through a false-discovery rate set to 1% at protein and peptide-sequence match level. The match level was determined by a target-decoy search using the in-house-developed Proline software version 1.6 (<http://proline.profi-proteomics.fr/>). The 1-DE gels were treated according to IPBS protocols for washing, trypsin digestion and drying. Dry peptide extract was taken in 14 µL of a 2% acetonitrile solution/0.05% trifluoroacetic acid. For MS analysis, 5 µL of peptide extract was injected and the rest was stored at -20°C until further use. The raw data were obtained after searching with Mascot Daemon search engine in the local data bank MicroMar (*Chlamydomonas* + *H. pluvialis* on SP/tremble; 03-18-2016). The created lists of proteins were validated using the Proline software. Briefly, the trypsin was used as a cleaving enzyme and one missed cleavage was allowed. The methionine oxidation has been defined as variable modification and carbamidomethylation of cysteines defined as fixed change. Data validation was performed with the Proline software. Peptides and proteins were confirmed by generating a random peptide Bank "decoy", where the threshold of false positives (FDR) has been set at 1% for peptides and proteins. The proteins identified with exactly the same set of peptides (samesets) or part of the same set of peptides (subsets) have been grouped in the form of lists in Excel tables. Proteins of the same group were classified according to their protein score, their number of peptide sequences (specific or non-protein), and their number of tandem mass spectrometry (MS/MS) fragmentation spectra. Only one member of the group has been moved in the list of the identified proteins; the protein of 1st row.

2.7. Statistical analysis for the biological studies

Each experiment was done in triplicate. Subsequent statistical analyses were performed using SPSS freeware (version 17.0). Means of two data sets were compared using unpaired Student's t-tests. The significance level was set at a p value < 0.05.

3. RESULTS

3.1. Characterization of the newly isolated strain

3.1.1. Taxonomic position

The morphological observations (Fig. S1-1 in supplemental data 1) allowed the identification of the new strain as *Haematococcus pluvialis* [12]. The 18S rRNA sequence of this strain was 99% identical to other 18S rRNA sequences of *H. pluvialis* and clusters with *H. pluvialis* and *H. lacustris* (Fig. S2-1 in supplemental data 2). These results are discussed in supplemental data 2.

3.1.2. Growth conditions of the identified *Haematococcus pluvialis* strain

Under autotrophic culture conditions (carbon source: NaHCO_3 (MLA medium) or Na_2CO_3 (BG11 medium)), the cell density remained constant throughout the incubation period. In contrast, a typical sigmoid growth curve was obtained with TAP medium under both mixotrophic (growth under low light intensity) and heterotrophic (growth in complete darkness) conditions. Under mixotrophic conditions, the growth rate (0.856 d^{-1}) was 48% higher than under heterotrophic conditions (0.577 d^{-1}). The highest cell density was also reached with mixotrophic conditions (after 8 days of growth) (Fig. 14). At that time, the palmella stage represented $60 \pm 10\%$ of the cells. The remaining 40% of the microalgae corresponded to the macrozoid stage (data not shown). The cell diameter ranged between 15 and $49 \mu\text{m}$ with a mean of $23 \mu\text{m}$. The distribution of the cell diameters among the microalgal population used for PEF treatment did not allow to distinguish two subpopulations (Fig. S2-1 in supplemental data 2).

Here is Figure 1.

3.2. Water-soluble protein extraction following different PEF treatments

The objective of the following experiments was to identify suitable PEF conditions (number of pairs of pulses and field strength) for the electro-extraction of water-soluble proteins. An overview of the global experimental approach is shown in Schematic 2.

Here is Schematic 2

Here is Figure 2

No significant difference in terms of extracted protein concentration was found between the negative control (i.e. no PEF procedure) and the control condition (0 kV cm^{-1}) (Fig. 2), suggesting that the shear forces linked to the use of a peristaltic pump did not provoke a significant release of proteins from the microalgae. Furthermore, because (1) the axenic tests were negative, and (2) the microalgae pellets of the negative control had been washed before its transfer to the low-conductivity PEF medium (i.e. distilled water), we can assume that the measured protein in both supernatants resulted from their diffusion out of the microalgae after their transfer to the PEF medium (maybe because of variations in osmotic pressure). Importantly, compared to these control conditions, the PEF treatments released a significantly higher amount of water-soluble proteins into the supernatant medium (Fig. 2). Specifically, after a PEF treatment at 1 kV cm^{-1} (which included the post-treatment incubation period of 45 min) we recovered 46% of the total recoverable proteins (as determined by destructive extraction through grinding with glass beads, i.e. the positive control). Interestingly, the application of a higher number of pulse pairs ($N=9$) did not significantly impact the amount of electro-extracted proteins (Fig. 2).

3.3. Identification of the electro-extracted proteins

The extracts prepared without or with PEF procedure (0.5 or 1 kV cm⁻¹) were used for protein determination. In this way we identified 52 proteins (Table 1) that could be ranged into 4 categories with respect to their predicted functional roles in the physiology of *H. pluvialis* (Table 2).

Here should be table 1

Here should be table 2

Proteins assigned as ‘Core metabolism proteins’ were those involved in the synthesis of lipids, proteins or photosynthesis. Detected ‘stress response proteins’ were those involved in the metabolism of reactive oxygen species or DNA protection (Table 2). The category of ‘cell movement proteins’ had functions in the cytoskeleton, flagella, or cell trafficking pathways are involved in cell motility and intracellular movements. Unassigned proteins included those that contained distinct domains or motifs but that had an unassigned cellular function. Nevertheless, on the basis of domain homologies, an identity could often be proposed for these proteins. Therefore, and for allowing the most comprehensive insights about the consequences of protein electro-extraction by PEF, these unassigned proteins will be discussed together with the other protein categories when possible.

The largest number of electro-extracted proteins belonged to the core metabolism protein category, constituting 55% of the soluble extracted protein (Table 2). Most of these proteins appeared to originate from the chloroplasts where they were involved in photosynthesis metabolism, or the synthesis of lipids, proteins or vitamin B6 (Table 1, supplemental data S3).

3.4. Impact of the PEF strength on the physiological status of the cell culture after a recovery period of 30 min

In order to address the question about the biocompatibility of the PEF treatment, we investigated its impact on the physiological state of the culture after a 30 min recovery period. During this period, the microalgae were incubated in their initial culture conditions (TAP medium, 35 μ moles of photons m⁻² s⁻¹).

Here is Figure 3

Four parameters were studied, i.e. cell motility (Fig. 3A), photosynthetic oxygen evolution (Fig. 3B), maximum quantum yield of PS II photochemistry (Fv/Fm ratio) (Fig. 3C) and respiration intensity (Fig. 3D). The comparison of values measured in the control condition (0 kV cm⁻¹) and those obtained from a standard 8 days-old culture indicated that neither the flow in the PEF chamber, nor the post-treatment incubation in distilled water, altered the physiological status of the culture (data not shown).

3.4.1. Macrozooid motility

Under our culture growth conditions, the proportion of macrozooids in the cultures was around 40%. The remaining cells were in the palmella stage (data not shown). In the control condition, the ratio between motile and nonmotile cells stayed unchanged (Fig. 3A). Regardless of the field strength, the PEF treatment significantly reduced the relative amount of motile cells. However, this reduction in cell motility was the strongest after PEF treatments of 0.5 and 1 kV cm⁻¹, yielding a reduction of 50% and 75% respectively. For higher PEF intensities (2, 3 and 6 kV cm⁻¹), the percentage of motile cells remained around 4%.

3.4.2. Photosynthetic and respiratory activities

Here is Figure 6

The photosynthetic oxygen evolution (Fig. 3B) and Fv/Fm ratio (Fig. 3C) showed a similar response to the PEF treatment condition: they first decreased and then reached a stationary level with field strengths greater than or equal to 1 kV cm⁻¹. At any field strength greater than 0.5 kV cm⁻¹ the values of both parameters were significantly different from the control condition. However, the PEF treatment impacted the oxygen evolution capacity (- 50%) more strongly than the maximum quantum yield of PS II (- 10%). Photosynthetic pigments were also electroextracted (Supplemental data 4). The application of a PEF of 1 kV cm⁻¹ resulted in a 22.5% reduction in the respiratory rate value (when compared to the control condition).

In conclusion, the results described in sections 3.2 and 3.3 indicate that the best compromise between protein extraction yield and microalgae survival is obtained with a 5 pairs of pulses and a field strength of 1 kV cm⁻¹.

3.4.3. Cell permeability and biocompatibility of the PEF-treatment

Without treatment and processing, the relative abundance of the NAT-P cell type was around 8 %, a value similar to those in the literature [8]. The cell processing increased this proportion by 300% (Table 3).

Here is table 3

The observed increase in the permeability of the plasmalemma in function of the field strength indicated the existence of two phases: a sharp increase from 0 to 1 kV cm⁻¹ followed by a smooth increase for strengths higher than 1 kV cm⁻¹ (Fig. 4A). Using equations 2 to 6, the relative abundance of the different cell categories were calculated (Table 3). Under the lowest field strength, the level of NA cells was the highest. It decreased sharply until 2 kV cm⁻¹ and then stabilized. The variations of RP cells presented a bell-shaped curve with an optimum between 2 and 3 kV cm⁻¹. Until the field

strength reached 2 kV cm^{-1} , the variations of IP cells followed the same trend as RP cells but instead of decreasing, the relative abundance of IP cells increased slightly above 2 kV cm^{-1} (Fig. 4B). The combination of the proportions of NA and RP cells allowed the definition of the BI. This index decreased from 0.5 to 2 kV cm^{-1} , then transiently stabilized before decreasing again. The highest field strength for which the BI was at least 50 % was 3 kV cm^{-1} (Fig. 4C).

Here is Figure 4

As expected by Equation 8, the total energy of the treatment, WPEF, increased with the PEF intensity and the number of pulses (Table 4). An energy input of 0.8 kJ kg^{-1} yielded the highest proportion of RP cells¹ (Table 4), while inputs higher than 3.34 kJ kg^{-1} resulted in BI values below 50 % (Table 4).

3.5. Evolution of the physiological state of PEF-treated cultures during a recovery period of 72 h

To get information about the cell recovery and the physiological state of the cultures, the cell division rates and motility of *H. pluvialis* was determined during the three days following their exposure to a PEF of 1 kV cm^{-1} (N=5). During this period, microalgae were transferred back to their initial culture conditions (TAP medium, $35 \mu\text{moles of photons m}^{-2} \text{ s}^{-1}$). The percentage of motile cells reached the value of the control condition within 2 days after the treatment (Fig. 5A). In both conditions, the relative amount of motile cells increased after the first day of the recovery period and continued to rise during the next two days, reaching a maximum proportion of 85% motile cells on day 3. In contrast to the motility, the cell division rate was only slightly lower in the treated cells (0.50 d^{-1}) compared to the untreated cells (0.63 d^{-1}), and the absolute cell densities were not significantly different between the conditions at any given day during the three days post-recovery (Fig. 5B).

Here is Figure 5

During the first two days of the recovery period, the values of the photosynthetic oxygen evolution (Fig. 5C) and the maximum quantum yield of PS II photochemistry (Fig. 5D) remained significantly lower in the treated cells compared to the untreated cells (0 kV cm^{-1}). However, from the third day post-recovery, the values of both photosynthetic oxygen evolution and Fv/Fm ratio of the PEF-treated cells increased to reach similar values to those of the untreated cells (Fig. 5C and 5D).

3.6. Optimization of the post-treatment incubation protocol

To improve the physiological state of the PEF-treated cells, the impact of a residence time reduction of cells in distilled water (i.e. a shortening of the incubation period, which was so far fixed at 45 min) was tested (Schematic 3, protocols 1 to 4) and compared to the protocol used so far (protocol 5). Treatments differed either by the length of the incubation period in distilled water (protocols 1, 2 and 3), the presence/absence of the first centrifugation step, i.e. the presence/absence of the recovery period (protocols 1 and 4), or by the composition of the fresh medium in which treated cells were transferred at the end of the incubation period (protocol 2). Physiological parameters as well as protein amounts were measured at specific steps during each protocol (Schematic 3).

Here is Schematic 3

Here is Figure 6

According to Fig. 6A, reduction of the time that cells spent in distilled water (i.e. 5 min instead of 45 min post-treatment) caused an 11% decrease in the electro-extracted protein yield. In contrast, a very small amount of proteins ($< 0.3 \mu\text{g mL}^{-1}$) was measured in the extracellular medium after cells were placed in fresh TAP medium for 30 min. We also found that the relative amount of motile cells did not change regardless of the protocol used (Fig. 6B), thereby suggesting that the transfer in fresh TAP medium only 5 min after the PEF treatment (protocol 3) did not cause any osmotic shock. Interestingly, the absence of the centrifugation step (and consequently the absence of mechanical stress to the cells) in protocols 1 and 4 had also no impact on the motility. Finally, we found that oxygen evolution (Fig. 6C) and the maximum quantum yield of PS II photochemistry (Fig. 6D) were improved by using protocol 3. Interestingly, the simple fact of returning the treated cells to their culture conditions (TAP medium, $35 \mu\text{moles of photons m}^{-2} \text{ s}^{-1}$) for 30 min (protocols 3 and 5) induced a significant increase in the values of both measured parameters. This improvement was independent of the time (5 or 45 min) that cells spent in distilled water before their transfer to TAP medium. Similar values for N-PEF cells were obtained 5 or 45 min after PEF delivery (Table 3).

4. Discussion

The main aim of this study was to provide a proof of concept for the use of pulsed electric fields in the biocompatible electro-extraction of internal compounds from microalgae. To this end, we have used a multidisciplinary approach, including biochemistry, proteomics and physiology. The major results are discussed in this section.

4.1. TCC932, a mixotrophic strain of *Haematococcus pluvialis*

Similarly to the *H. pluvialis* NIES-144 strain [23], the best growth conditions for the newly identified TCC932 strain were low photon flux densities and the presence of acetate-containing (TAP) medium as an external carbon source, which is in accordance with the identified phylogenetic proximity of these two strains (Fig. S1-2 in Supplemental Data 1). Interestingly, under heterotrophic conditions the growth rate of the strain TCC932 was higher than that obtained under autotrophic conditions, whereas an opposite result was obtained with *H. pluvialis* NIES-144 [23]. To explain this difference, we suggest that in our mixotrophic culture conditions the performance of strain *H. pluvialis* TCC932 was mainly based on heterotrophy. This may explain the higher growth rate of the strain TCC932 under mixotrophic conditions when compared to the literature data, whatever the mode of nutrition (e.g., [24]).

4.2. The yield of protein extraction using PEF treatment is high

Using the TCC932 strain, the protein extraction efficiency was not linearly related to the field strength: it increased constantly and significantly for PEF strengths up to 1 kV cm^{-1} (by 5-fold when compared to the control condition) and then tended to stabilize. These results differ from those reported in [6] which showed that the protein extraction yield from *H. pluvialis* increased significantly with field strengths between 3 and 4.5 kV cm^{-1} . The reason for this divergence remains unclear but could lie in the difference in the algal strain used [6, 19]. Besides the cell size, the presence of a rigid cell wall could affect the treatment efficiency [25]. Electrical pulses can cause the appearance of electromechanical forces, which are maximal when cells are suspended in a low-conductivity medium [18]. Therefore, the extraction yield could vary depending on the capacity of the cells to resist these forces (which likely depends on the properties of the cell wall). Alternatively, this difference could also be explained by a difference in axenicity between the two strains. For the TCC932 strain, in addition to negative axenic tests (data not shown), no bacterial protein were detected in the supernatant by proteomic analysis (see sections 3.6 and 3.7). The yield of protein recovery by grinding after the post-treatment incubation period reached 46% of the water-soluble, extractable proteins. A similar yield was found by Coustets, Al-Karablieh, Thomsen and Teissié [19] with the microalga *Nannochloropsis salina* (Eustigmatophyceae) using 2 ms bipolar pulses with an intensity of 6 kV cm^{-1} . However, these yields are much higher than those reported by authors working on other microalgae species. For example, using a length of 5 μs for each monopolar square pulse, Postma, Pataro, Capitoli, Barbosa, Wijffels, Eppink, Olivieri and Ferrari [26] reached only a yield of 10% using the green microalga *C. vulgaris* and a much stronger PEF strength (17.1 kV cm^{-1}). Therefore, besides pulse intensity, pulse duration also appears to be an important parameter for optimizing the extraction yield. Interestingly, the same trend was obtained with both numbers of pairs of pulses ($N=5$ or 9) because an increase of this parameter value (from 5 to 9) did not significantly impact the amount of electro-extracted proteins (Fig. 2). In our case, this appears to suggest that the number of paired pulses has no additional effect on the degree of permeabilization of the plasma membranes. An interesting aspect of our work consists of estimating the amount of extracted protein if the PEF process would be implemented in an actual *Haematococcus* production plant. The major

technologies used for growing algal biomass are the low-cost, open raceways and the more expensive, closed photobioreactors (PBR) [27]. The latter production system is used for growing *Haematococcus* biomass for astaxanthin production. For this purpose, Li, Zhu, Niu, Shen and Wang [28] combined two large scale outdoor PBRs of 1000 and 8000 L, respectively to several raceway ponds. The working cell density in the PBR (5×10^5 cells mL⁻¹) was similar to the one used here (10^5 cells mL⁻¹) making a dilution step before the PEF treatment unnecessary. In our work, the yield of electro-extracted proteins was 12 µg mL⁻¹ (Fig. 1) which corresponds to a mean mass of 0.12 ng protein per cell. A simple calculation indicates that more than 480 g of proteins could be harvested per 8000 L. Another example is the PBR of 25000 L which produced 0.36 g of *Haematococcus* DW L⁻¹ [29]. Taking into account the assumption that a single *Haematococcus* cell weighs 10^{-9} g DW [29], one can calculate that 1080 g protein could be extracted from this volume. This value is coherent with the amount that would be obtained with the 8000 L PBR.

4.3. The electro-extracted proteins are involved in many vital cell processes

The predicted MW of the electro-extracted proteins ranged from 12.4 to 164.9 kDa. The range of extracted proteins is higher than the one reported by Postma, Pataro, Capitoli, Barbosa, Wijffels, Eppink, Olivieri and Ferrari [26]. One could be surprised that high MW proteins were retrieved through PEF extraction. However, it is known that proteins as large as 98 kDa can be imported using a PEF treatment [30]. Using the procedures developed in our study, nearly 50% of the electro-extracted proteins originated from chloroplasts. In addition, the diversity of proteins in P_{1.0} was higher than in P_{0.5} due to an increase of the permeation of the different cell compartments (Supplemental data 3). This result contrasts greatly with the results of [31] which displayed a destructive impact of PEF treatments, resulting in the extraction of mostly cytosolic proteins [31]. So far, we do not have a real explanation for this difference. A hypothesis would be that PEF treatment induced a phase separation in the cytoplasm, somehow slowing down the cytoplasmic protein extraction. Cytoplasmic phase separation consists in a transient aggregation of proteins forming gel-like structures [32]. Alternatively, one can suggest that in our conditions, the presence of cell compartments, such as the ER network, resulted in the hindrance of the mobility of cytoplasmic proteins and therefore could reduce the conductivity of the cytosol [33]. The next subsections discuss the proteins found within each of the categories defined in Table 2.

4.3.1. Cell and cellular movements

As observed with rotifers [34], PEF treatment impaired the motility of *H. pluvialis*. The reduction in both respiration and photosynthesis, which decreases of cellular ATP production, could be responsible for this decrease in cell motility. *Haematococcus* is a bikont organism, i.e. it has two flagella that are used to move. The locomotive system can roughly be divided in two parts, i.e. the flagella in itself and the basal body, which constitutes the machinery moving the flagella. Each basal body has four-membered microtubules and a two-membered microtubule rootlet. Only the latter contains acetylated α -tubulin [35], which is a protein that we found among the electro-extracted proteins. Mass spectrometry analyses (Table 1) also revealed the presence of β -tubulin proteins. α - and β -tubulins are part of the cytoskeleton playing a central role in many

cell functions such as cell shape, cell division and motility. Tubulins also play an important role during the cell cycle because they assemble into the microtubules that form the mitotic spindle [36]. Another electro-extracted protein, the AAA-ATPase CDC48, belongs to the flagella-associated proteins [37] (Supplemental Data S3). Recent results suggest that CDC48 is mostly involved in disassembling flagella and segregating ubiquitinated molecules from protein complexes and cellular structures [38]. CDC48 has also been found to play a role in the regulation of cell-cycle progression in plants [39]. Interestingly, in the land plant *Arabidopsis*, CDC48 can form complexes with several other proteins, including GF14k, a 14-3-3 protein that is known to prevent cytokinesis [40]. The data presented in Fig. 10, which showed that the cell division rate was not significantly affected by the PEF treatment, might suggest that CDC48 and/or its complex with 14-3-3 proteins only acted on cell motility and not cell division.

4.3.2. The photobiochemical phase of photosynthesis

The PEF treatment was also affecting the functioning of cell organelles and especially that of the chloroplast. In green algae, the chloroplast is limited by a double envelope that surrounds the stroma. The stroma contains the so-called thylakoids, which are the membranes that host the photosynthetic apparatus. In green algae, the thylakoid membranes are organized in stacks (grana) that are interconnected by stroma-exposed lamellae. The photosynthetic machinery is composed of four macro-complexes, namely the PSII, the cytochromes b_6/f , PSI, and the H^+ -translocating ATP synthase (CF_0F_1). The PSII is composed of the photosynthetic reaction center and a light-harvesting antenna complex, including the chlorophyll *a* binding protein CP43 [41]. In *Chlamydomonas*, the CP43 protein structure overlaps with that of PsbO [42], a 33 kD protein that is involved in maintaining and stabilizing the manganese cluster of water oxidase [43]. In the *Chlamydomonas* mutant strains F23 and FuD44, PsbO is lacking and this results in a dysfunctional PSII complex [44] and an absence of oxygen evolution [45], respectively. The electro-extraction of these two proteins in our experiments could be responsible for the dramatic decrease of the oxygen evolving capacity of PEF-treated cells. Electro-extracted chlorophyll *a* and carotenoids could originate from their association with the electro-extracted CP43 protein, but because CP43 does not contain chlorophyll *b*, this pigment should have originated from (an)other pigment-binding protein complex(es) composing the light-harvesting antenna. Altogether, these data suggest a partial impairment of light harvesting and of the capacity to generate oxygen. The apparent discrepancy between the reduction of the oxygen evolution capacity (- 50%) and the maximum quantum photochemical yield of PS II (- 10%) can be explained by the fact that the oxygen release measurements were performed with light-adapted samples whereas the Fv/Fm ratios were calculated using dark-adapted samples. The weak impact of the PEF treatment on the maximum quantum yield of PSII photochemistry was also observed previously [46] and it was asserted that a decrease of the Fv/Fm value from 0.71 to 0.61 was not indicative of significant cell stress. The decrease of the photosynthetic activity values may be partly due to disturbances in the photosynthetic electron transport chain [46], either through charge accumulation on the membranes [33, 46] or due to a reduction in the availability of electron transport proteins, such as the ferredoxin:NADP⁺ reductase (E.C. 1.18.1.2) (FNR) which catalyses the reduction of NADP⁺ to NADPH at the stromal side of PSI.

Therefore, the electro-extraction of FNR in our experiment might have affected the availability of NADPH, which is an essential electron donor for carbon dioxide fixation by the Calvin-Benson-Bassham cycle (CBB cycle) (see 4.3.3). Furthermore, the electron flow through the thylakoid membranes is accompanied by the transport of protons from the stroma to the thylakoid lumen, generating an electrochemical gradient across these compartments. The free energy associated with this gradient is coupled to the synthesis of ATP by the ATP synthase enzyme complex. The general structure of ATP synthase comprises a membrane spanning subcomplex, denoted F_0 and a soluble component, denoted F_1 . Proteins identified as α - and β -subunits of the CF_1 subcomplex of ATP synthase are among the electro-extracted proteins (Table 1 and Supplemental data 3), suggesting that the PEF treatment would reduce the capacity of chloroplasts to generate ATP.

4.3.3. The biochemical phase of photosynthesis

The putative reduction in the production capacity of ATP and NADPH in the photobiochemical phase of photosynthesis can be expected to impact the production of triose phosphate by the CBB cycle. Therefore, the cell's production capacity of simple sugars, which are either used as an immediate energy source, or for the synthesis of larger cellular building blocks, is likely also reduced. This effect can be expected to be further enhanced by the observed electro-extraction of three proteins of the CBB cycle, namely phosphoribulokinase (E.C. 2.7.1.19), glyceraldehyde-3-phosphate dehydrogenase (E.C. 1.2.1.12) and the large subunit of RuBisCO (E.C. 4.1.1.39) (Supplemental data 3). Of these, phosphoribulokinase catalyzes the ATP-dependent phosphorylation of ribulose 5-phosphate to ribulose-1,5-bisphosphate, which is the CO_2 acceptor molecule, and a substrate of RuBisCO. RuBisCO is an abundant plant enzyme composed of several large (catalytic, 55 kDa) (LSU) and small subunits (SSU) (15 kDa) which together form a massive hexadecameric protein complex with a molecular mass of about 550,000 Da [47]. Active enzymes are exclusively localized in the pyrenoid [48], but RuBisCO subunits are also found in the chloroplast stroma [49]. The extraction of active RuBisCO using PEF in destructive mode has been reported earlier [49]. In our work, only the large RuBisCO subunit, i.e. the one encoded in the chloroplast's DNA, has been found among the electro-extracted proteins (Supplemental data 3). We can hypothesize that these subunits do not arise from functional RuBisCO but from a storage or degradation pool of LSU. This hypothesis is likely because Recueno-Muñoz, Offre, Valledor, Lyon, Weckwerth and Wienkoop [50] found that the LSU/SSU ratio can be as high as 5 in the green alga *Chlamydomonas reinhardtii*. A LSU/SSU ratio of 1 is required for functionality and higher ratio's are known to result from the accumulation of a LSU degradation product (37 kDa). The fact that Hsp70 proteins were found among the electro-extracted proteins is also an argument in favor of this hypothesis because these proteins cooperate with the chaperonin 60B2 to affect protein folding, including the folding of RuBisCO [51]. Because RuBisCO is the rate limiting protein in the carbon fixation process, a reduction of its amount may thus have reduced the capacity of the algae to recover after the electro-extraction treatment.

Another extracted protein, glyceraldehyde-3-phosphate dehydrogenase, catalyzes the transformation of 1,3-diphosphate glycerate to D-glyceraldehyde-3-phosphate, a key

metabolite of the CBB cycle and the glycolysis. In addition, the extracted phosphoribulokinase enzyme (Supplemental data 3) is mostly predicted to be localized in the chloroplast where it would interact with adenylate kinase (ADK). This interaction was recently found to constitute a regulatory mechanism responsible for optimizing the functioning of the CBB cycle [52]. Altogether, the putative slowing down of the CBB cycle by the electro-extraction, may thus decrease the utilization of NADPH. An important consequence of this might reside in the acceleration of the production of the reactive oxygen species hydrogen peroxide (H_2O_2) [53]. Because H_2O_2 has the ability to readily permeate membranes, its elevation likely impacts the functioning of both chloroplast and nuclear-encoded proteins [54]. Given that the permeation of membranes is further enhanced by the PEF treatment [55], this hypothesis is especially interesting because H_2O_2 might impair PSII repair [56] during the PEF recovery period (see also 4.3.6; oxidative stress) (Schematic 3).

4.3.4. Lipid biosynthesis

Lipids are important cell building blocks that under non-stressful conditions, are recruited to build membranes, to accommodate cell signalling, or to generate energy. Under stressful conditions, however, large amounts of triacylglycerol (TAG) can accumulate because of the diversion of fatty acids (FA) from membrane lipid synthesis to the synthesis of TAG, and/or by converting preformed membrane lipids to TAG [57]. Biosynthesis of lipids in algae encompasses two parallel pathways within multiple subcellular compartments, including the chloroplast. Our analyses revealed the electro-extraction of the chloroplast enzyme, acyl carrier protein (ACP). ACP acts as a carrier of FA at the end of the FA biosynthesis pathway. The FAs are subsequently processed by either stearoyl-ACP desaturase, generating 18:1-ACP, and/or by acyl-ACP thioesterases mediates the release of the FA from the ACP carrier. Because Lei, Chen, Shen, Hu, Chen and Wang [58] proposed that ACP is a key rate-limiting protein in FA synthesis, the electro-extraction of this enzyme may slow down FA production by the microalgae.

Electro-extraction of another enzyme, argininosuccinate synthase (EC 6.3.4.5), might further contribute to a reduction in FA biosynthesis after PEF-treatment. The reason for this relates to the ability of the N-containing molecule urea to induce FA synthesis in *Chlamydomonas*, even in the absence of cell stress [61]. Urea is typically produced by the ornithine-urea cycle, a metabolic pathway in which argininosuccinate synthase catalyzes the synthesis of argininosuccinate from citrulline. Although a functional urea cycle has not (yet) been identified in *H. pluvialis*, the amino acid arginine can be catabolized to citrulline in *Chlamydomonas* [59]. Therefore, even in the absence of an ornithine-urea cycle, the electro-extraction of argininosuccinate synthase can be expected to reduce urea production and consequently hamper the synthesis FAs in *H. pluvialis*.

4.3.5. Protein biosynthesis and trafficking

We detected several electro-extracted proteins that are functionally involved in the cell's protein production pathway. In all organisms, ribosomes are responsible for the translation of mRNA into proteins. However, due to their endosymbiotic history, eukaryotic cells like *H. pluvialis* have ribosomes of prokaryotic origin in their chloroplasts and mitochondria. These ribosomal complexes consist of a large subunit

(50S) and a small subunit (30S), both of which contain ribosomal RNAs and various ribosomal proteins. We found that the PEF treatment extracted several of these proteins from the chloroplasts and mitochondria (Supplemental data 3), for example two L7/L12-like proteins [60]. The concentration of ribosomes in cells correlates with cell division rates because the cell's rate of protein production needs to increase when the cell division rate increases. The electro-extraction might thus have impacted the observed decrease in cell division rate [61].

In *Chlamydomonas*, 10-40% of the chloroplast ribosomes are associated with membranes by electrostatic interactions alone [62]. The detection of chloroplast ribosomes in the electro-extracted protein pool thus suggests that electro-extraction might disturb these electrostatic interactions. This insight opens new avenues for the study of the inter-molecular mechanisms underlying the electro-extraction of proteins from eukaryotic cells.

Among the electro-extracted proteins the protein TufA and the eukaryotic translation elongation factor 1 alpha (EF-1a) were also identified (Supplemental data 3). TufA is a protein that is encoded in the chloroplast genome [63] and it functions together with EF-1a during the binding of elongator aminoacyl-tRNAs to the A site of mRNA-programmed ribosomes [64]. Besides this crucial role, TufA likely plays additional roles in protein synthesis and in the control of protein synthesis quality [65]. To be active, proteins must be folded. Similarly, EF-1a may exert roles in coordinating regulation of multiple cellular processes including growth, and division [64]. For example, EF-1a may compete with the beta subunit of the nascent polypeptide-associated complex, another electro-extracted protein and with protein #47 predicted as having this domain (Supplemental data 3). The interactions between the two latter proteins constitute a molecular mechanism modulating mRNA translation *in vivo* [66]. Most of nascent proteins enter the endoplasmic reticulum (ER) where they are folded by chaperones. Among them, the luminal binding protein BiP, an electro-extracted HSP70 molecular chaperone.

Targeting the proteins to the adequate compartment is a crucial mechanism for optimal cell functioning. An ADP-ribosylation factor 1 (Arf1-like), which belongs to the superfamily of small GTPases, was found among the electro-extracted proteins. In land plants, Arf1 is targeted to the Golgi and post-Golgi structures, two subcellular structures specialized in protein targeting [67]. Arf proteins are also targeted to other cell compartments, including peroxisomes and lipid droplets [68]. To date there is no data about this in *Haematococcus*, nor in *Chlamydomonas*. Therefore, a follow-up study using electron microscopy on algae treated with PEF could provide important information on the Golgi apparatus structure and consequently on the mechanisms involved in the recovery from PEF treatment. The protein import into mitochondria and chloroplasts is more diverse and more complex than for other cell compartments. The uncharacterized protein #49 contains a Gene Ontology (GO) domain annotation as non covalent binding typical of HSP90A, a chloroplastic protein coded by a nuclear gene and involved in protein import in *Chlamydomonas* chloroplast [69]. Once imported to the chloroplast, the proteins should be adequately folded by chaperonin proteins. One of these proteins, the uncharacterized protein #50 (Supplemental data 3), has a GO annotation that indicates ATP binding site of a protein involved in protein refolding

such as GroEL-like protein, a central protein member of the chloroplast chaperonin system [70].

Uncharacterized protein #48 contains a GO annotation (GO: 0005524) that suggests a function in noncovalent ATP-binding as exhibited by the chloroplastic ClpA/ClpB family of proteases. These proteins are involved in protein turnover and several of them have been identified in land plant chloroplasts. Among them, ClpC, the plant homolog of bacterial ClpA, has a MW of 100 kDa [71] which is very close to the MW of detected protein #48 (Supplemental data 3).

Two S-adenosylmethionine synthases (EC 2.5.1.6) were also electro-extracted (Supplemental data 3). They catalyze the formation of S-adenosylmethionine (SAM) from methionine and ATP [72]. SAM serves as a methyl donor for transmethylation in many biosynthetic pathways, such chlorophyll biosynthesis and phytohormone biosynthesis. Because DNA methylation is an important factor controlling gene expression, these enzymes could also be important elements in the establishment of microbial stress responses – similar to their action in plants [73].

4.3.6. Stress response proteins

Nucleic acids

RNA helicases are RNA degradosome enzymes that are involved in every step of RNA metabolism, including nuclear transcription, pre-mRNA splicing, ribosome biogenesis, nucleo-cytoplasmic transport, translation, RNA decay, and organellar gene expression, including the disruption of misfolded RNA structures [74]. Here, we report for the first time a DEAD-box helicase (protein #17) from *H. pluvialis* that is homologous to the *Chlamydomonas reinhardtii* CiRH4 for which the role remains elusive. The electro-extraction of DEAD-box RNA helicases can be due to the salinity change that the algae underwent before PEF treatment. Additional experiments have to be performed to validate this hypothesis. Interestingly, the uncharacterized protein #52 also belongs to the DEAD box helicase family of proteins.

Oxidative stress

The formation of reactive oxygen species (ROS) is inherent to cellular processes, e.g. photosynthetic electron transport. ROS can participate in cell signalling and can modify enzyme activities, which for example can result in the activation of the oxidative pentose phosphate pathway [75]. ROS formation is associated to PEF treatment. Indeed, Bai, Gusbeth, Frey and Nick [76] showed that nanosecond PEF generated an oxidative burst that can last several days in *Chlamydomonas reinhardtii*. Fortunately, to keep the oxidative risk at an acceptable level, cells have an arsenal of detoxifying enzymes at their disposal, such as superoxide dismutase (SOD).

The finding of one SOD (with predicted cytoplasmic targeting; supplemental data S3) in the electro-extracted protein pool may thus transiently increase the risk for oxidative damage. A likely scenario is that the generated ROS reacts with the head groups of plasma membrane phospholipids. An *in silico* study has predicted this will result in an overall decrease of the free energy barriers that normally limit membrane permeation

(i.e. an increase of the membrane permeability to ROS) [55]. However, this increase would not be sufficient to allow an easy export of ROS scavengers. In addition, lipid oxidation could decrease the average time needed to initiate pore formation, which in the case of repetitive treatment, such as proposed in a milking protocol [4], could constitute an advantage. Beside their oxidative properties, a decrease in the intracellular ROS scavenging capacity would thus intensify signalling, which in turn might be responsible for the macrozoid-to-palmella transition and/or the adaptation to osmotic stress [76].

Signal transduction

The 14-3-3 proteins are well-known for their involvement in signal transduction events. In the green alga *Chlamydomonas*, the protein has been reported in 4 cell compartments: the ER (27 kDa), the Golgi apparatus (23 kDa), the plasma membrane (23 kDa) and the cytosol (30 kDa) [77]. The deduced MW of the electro-extracted 14-3-3 proteins are close to 30 kDa or 27 kDa and the *in silico* predictions of their subcellular localization suggest the extraction from ER and cytosol.

4.3.7. Proteins with miscellaneous actions

Protein #46 in Supplemental data 3 contains a gene ontology (GO) domain (GO:0042823) that is typically present in pyridoxal 5'phosphosphate synthases. Because pyridoxal 5'phosphosphate is a cofactor for many biochemical pathways, a reduction of the biosynthetic capacity may slow down many pathways such as chlorophyll biosynthesis [78]. Uncharacterized protein #51 contains a GO domain that is typical for enzymes within the phosphohexomutase superfamily. These enzymes are essential for carbohydrate biosynthesis.

Altogether, the presence of proteins involved in metabolic networks suggests that the recovery of the electro-extracted proteins may have a dampening effect on the cell and might provide an explanation for the observed lag phase during the recovery of the physiological properties of the PEF-treated algae (Fig. 10).

4.4. Biocompatible electroextraction: the proof of concept

The electric pulse during PEF treatment induces a large difference in electric charge across the plasmalemma which causes the formation of pores; the size of these pores is dependent on the pulse duration and the field amplitude [79]. In the event of reversible pore formation, the plasmalemma reseals approximately 30 s after the permeabilization [8], which allows cells to survive the electric treatment. However, following a PEF treatment, several types of cells coexist within the treated sample: RP cells, IP cells, NAT-P cells, NA cells, and cells that were permeabilized because of the cell processing such as those provoking shears stress (N-PEF). In this study, we estimated the size changes of these subpopulations for each tested field strength. The trends of the changes agreed with those reported in [8], e.g. the variation in the size of the RP subpopulation presented a bell-shaped curve with a maximum between field strengths of 2-3 kV cm⁻¹. Above this value, the relative abundance of IP cells increased. Based on these analyses,

we were able to define a biocompatibility index (BI) for the first time. At a field strength over 3 kV cm^{-1} , the BI was lower than 50% but at 1 kV cm^{-1} , the BI reached nearly 70%. It is important to note that the IP cell estimation was based on the assumption that the measured reduction in oxygen evolution was only due to cell death. However, as explained above, the reduction in oxygen evolution could also have arisen from a loss of photosynthesis proteins during electro-extraction. Thus, these cells are counted as IP while they belong to the RP category. Consequently, IP and RP values are probably overestimated and underestimated, respectively. Altogether the BI values would also be underestimated. As additional proof for the biocompatibility concept, the motility as well as the photosynthetic and respiration activities were followed after the PEF treatment. Because all these parameters returned to the level of the control cells within 3 days, the developed PEF procedure can be considered complete biocompatible. This implies that during the recovery phase, the PEF-treated cells repaired the damaged flagellar machinery and/or that new flagellated cells appeared through cell division. However, because the increase of cell density and the amount of motile cells in the control and PEF-treated conditions were proportional to each other, an alternative hypothesis seems more likely: the relatively slow rate of recovery (72 h) of the photosynthetic machinery is probably linked to the *de novo* synthesis of the electro-extracted molecules leading to a repair of the photosynthetic electron transport chain. It can, however, not be excluded that during the PEF treatment, one or more subpopulations are killed. Nevertheless, this possibility appears unlikely because the distribution of the diameters was symmetric around the $22 \mu\text{m}$ mean (Fig. S2-1 in Supplemental data 2).

Protein diffusion from PEF-treated cells was reported to occur up to 2 h after the treatment [19]. In our conditions, the amount of released proteins was not significantly different after an incubation period of 5 or 45 min, suggesting a fast protein diffusion out of the cells. This also implies that the pores created by the electric treatment have resealed within 5 min, which is in line with the reported pore resealing time of 30s [8]. Indeed, protocol 3 allowed photosynthesis and respiration to recover faster. This might be because PEF-treated cells were returned to TAP medium, which would allow the restoration of several ionic pools, including those required for an optimized photosynthesis process (Mg^{2+} , Cl^- , Ca^{2+} , phosphate and carbonate) [80]. It is clear that several mechanisms concur during protein electro-extraction, and to answer the above question further research is required that focuses on the phenomena occurring at the membrane level during and after the PEF treatment (e.g. charge accumulation, membrane potential).

In 2012, Chemat [81] defined 6 principles to which an extraction process must conform to be environmentally sustainable. Our biocompatible electroextraction of proteins meets most of them:

- *Principle 1 - Innovation by selection of varieties and use of renewable plant resources*: in this work, a new strain of *H. pluvialis* has been reported and used. Microalgae are well established as a renewable resource. The optimization of the PEF parameter allowing the biocompatible extraction of biomolecules opens new avenues toward microalga milking, which constitute a renewable process.

- *Principle 2 – Use of alternative solvent and principally water of agro-solvent:* the growth and extraction media are mostly aqueous solutions
- *Principle 3 - Reduce energy consumption by energy recovery and using innovative technologies:* Electro-extraction is a low-energy process that is based on diffusion in water. In addition, the implementation of biocompatible electroextraction in blue biotechnological processes, which aim the production of biomolecules, allows additional energy reduction [4]. The energy requirement could be even more reduced by decreasing the pulse duration.
- *Principle 4 – Production of co-products instead of waste to include the bio- and agro-refining industry:* The dead cells together with the excess cells produced by the continuous growth, can be processed and refined, for instance with the goal to extract pigments.
- *Principle 5 – Reduce the unit operation cost and favour a safe, robust and controlled process:* the implementation of a biocompatible PEF treatment unit as a part of a biotechnological process may reduce the complexity of the downstream processes because the biomass does not have to be harvested and does not have to be treated separately from biomass obtention. In addition, one can also envision an effect on the upstream parts of the process, because the treated cells recovered fast and, therefore, the whole biomass does not have to be regrown.
- *Principle 6 – Aim for a non-denatured and biodegradable extract without contamination:* the selectivity of the process has been demonstrated. The extract contains *circa* 50% of the soluble proteins, among which 52 proteins have been identified. The electrophoretic study suggests that these proteins were not degraded.

5. CONCLUSIONS

Current biotechnological processes rely on PEF treatment of microalgae with the aim to improve the extraction yield regardless of the viability of the treated cells. There is a need to develop more eco-friendly biotechnological processes, such as milking, but this necessitates the development of a biocompatible procedure [4]. Based on our results, the implementation of our biocompatible electro-extraction approach in a biotechnological process could effectively yield 25 µg proteins per mL culture medium. Furthermore, our method for the biocompatible electro-extraction of proteins meets most of the principles needed to be accredited as a green/eco-friendly/environmentally sustainable process. It opens the prospect of co-culturing microalgae and bacteria, where bacteria feed off the electro-extracted proteins that are synthesized through photosynthetic carbon fixation by the microalgae. The bacteria could then be used to generate biofuel [82]. Furthermore, the N-compounds released during the biofuel production process, such as ammonium, could be used as the prime nitrogen source to grow the algae [83]. Alternatively, the proteins could be harvested and refined into a high-value product. For example, the identification of the electro-extracted proteins has revealed the presence of enzymes with a high commercial interest, such as SOD, an anti-oxidative enzyme that is used for instance in the production of cosmetics. The PEF-based electro-extraction

procedure also be valorized by periodically electro-extracting the biomass of continuous microalgal culture and marketing the complete pool of extracted proteins for their nutritional values (Supplemental data 3). Finally, from a fundamental scientific standpoint the identification of the electro-extracted proteins also opens a new avenue for deciphering the modes of actions of PEF in living cells. Insights on the molecular mechanism driving the selectivity of the process will help support further innovation.

COMPETING INTERESTS STATEMENT: No

DECLARATIONS OF INTEREST: none

AUTHOR CONTRIBUTIONS: conceptualization, HG, JM and BS; methodology, VB, BV; validation, JM, VB and BS; formal analysis, HG, BV, OBS, CP, AG, JM and BS; investigation, HG, VB, BV, OBS, CP, AG; resources, JM and BS; data curation, OBS, CP and AG; writing—original draft preparation, HG; writing—review and editing, HG, CP, VB, JM and BS; supervision, JM, VB and BS; project administration, BS; funding acquisition, JM, VB and BS

ACKNOWLEDGEMENTS

The authors are grateful to Dr F Denis (Muséum National d'Histoire Naturelle, UMR BOREA, Station de Biologie Marine de Concarneau, France) for her help with the phylogenetic analysis and to Dr J Gillard (Department of Biology, California State University, Bakersfield, USA) for his critical reading of the text. The authors also thank the anonymous reviewer for their constructive comments.

FUNDING

HG thanks ‘Les Collectivités locales de la Sarthe’ for her PhD grant. The authors thank the doctoral school VENAM, the ‘College doctoral’ of Le Mans University and the University of Le Mans for their financial supports. This project was supported in part by the Région Midi-Pyrénées, European funds (Fonds Européens de Développement Régional, FEDER), Toulouse Métropole, the French Ministry of Research with the Investissement d’Avenir Infrastructures Nationales en Biologie et Santé program (ProFI, Proteomics French Infrastructure project, ANR-10-INBS-08) and by the Institut Universitaire “Mer Littoral” (IUML- – FR 3473 CNRS).

REFERENCES

- [1] M.M. Bomgardner, Protein evolution. Food trends combine with health and environmental concerns to put plant proteins in the spot light, *C&EN*, 2015 (2015) 8-13.
- [2] V. Mimouni, L. Ulmann, V. Pasquet, M. Mathieu, L. Picot, G. Bougaran, J.-P. Cadoret, A. Morant-Manceau, B. Schoefs, The potential of microalgae for the production of bioactive molecules of pharmaceutical interest, *Current Pharmaceutical Biotechnology*, 13 (2012) 2733-2750.
- [3] I.S. Chronakis, M. Madsen, Algal proteins, in: G.O. Phillips, P.A. Williams (Eds.) *Handbook of Food Proteins*, Woodhead Publishing, Philadelphia, 2011, pp. 353-394.
- [4] V. Vinayak, K.M. Manoylov, H. Gateau, V. Blanckaert, J. Herault, G. Pencreac'h, J. Marchand, R. Gordon, B. Schoefs, Diatom milking: a review and new approaches, *Marine Drugs*, 13 (2015) 2629-2665.

- [5] T. Kotnik, W. Frey, M. Sack, S. Haberl Meglic, M. Peterka, D. Miklavcic, Electroporation-based application in biotechnology, *Trends in Biotechnology*, 33 (2015) 480-488.
- [6] M. Coustets, V. Joubert-Durigneux, J. Hérault, B. Schoefs, V. Blanckaert, J.-P. Garnier, J. Teissié, Optimization of proteins electroextraction from microalgae by a flow process, *Bioelectrochemistry*, 103 (2014) 74-81.
- [7] A.A.b. Azmi, R. Sankaran, P.L. Show, T.C. Ling, Y. Tao, H.S.H. Munawaroh, P.S. Kong, D.-J. Lee, J.-S. Chang, Current application of electrical pre-treatment for enhanced microalgal biomolecules extraction, *Bioresource Technology*, 302 (2020) 122874.
- [8] P. Bodénès, S. Bensalem, O. Français, D. Pareau, B. Le Pioufle, F. Lopes, Inducing reversible or irreversible pores in *Chlamydomonas reinhardtii* with electroporation: Impact of treatment parameters, *Algal Research*, 37 (2019) 124-132.
- [9] C. Chen, S.W. Smye, M.P. Robinson, J.A. Evans, Membrane electroporation theories: a review, *Medical and Biological Engineering and Computing*, 44 (2006) 5-14.
- [10] S. Boussiba, Carotenogenesis in the green alga *Haematococcus pluvialis*: cellular physiology and stress response, *Physiologia Plantarum*, 108 (2000) 111-117.
- [11] F. Ba, A.V. Ursu, C. Laroche, G. Djelveh, *Haematococcus pluvialis* soluble proteins: Extraction, characterization, concentration/fractionation and emulsifying properties, *Bioresource Technology*, 200 (2016) 147-152.
- [12] P. Bourrelly, Les Algues vertes, N. Boubée et Cie, Paris, 1966.
- [13] J.J. Doyle, J.L. Doyle, Isolation of plant DNA from fresh tissue, *Focus*, 12 (1990) 13-15.
- [14] G.W. Saunders, D. Potter, M.P. Paskind, R.A. Andersen, Cladistic analyses of combined traditional and molecular data sets reveal an algal lineage, *Proceedings of the National Academy of Sciences of the United States of America*, 92 (1995) 244-248.
- [15] C.J.S. Bolch, S.I. Blackburn, Isolation and purification of Australian isolates of the toxic cyanobacterium *Microcystis aeruginosa*, *Journal of Applied Phycology*, 8 (1996) 5-13.
- [16] R.Y. Stanier, R. Kunisawa, M. Mandel, G. Cohen-Bazire, Purification and properties of unicellular blue-green algae (order *Chroococcales*), *Bacteriological Review*, 35 (1971) 171-205.
- [17] D.S. Gorman, R.P. Levine, Cytochrome f and plastocyanin: their sequence in the photosynthetic electron transport chain of *Chlamydomonas reinhardtii*, *Proceedings of the National Academy of Sciences of the United States of America*, 54 (1965) 1665-1669.
- [18] J. Teissie, M. Golzio, M.P. Rols, Mechanisms of cell membrane electropermeabilization: a minireview of our present (lack of?) knowledge, *Biochimica et Biophysica Acta*, 1724 (2005) 270-280.
- [19] M. Coustets, N. Al-Karablieh, C. Thomsen, J. Teissié, Flow process for electroextraction of total proteins from microalgae, *Journal of Membrane Biology*, 246 (2013) 751-760.
- [20] B. Schoefs, F. Franck, Chlorophyll synthesis in dark-grown pine primary needles, *Plant Physiology*, 118 (1998) 1159-1168.
- [21] K. Roháček, M. Bertrand, B. Moreau, J. Jacquette, C. Caplat, A. Morant-Manceau, B. Schoefs, Relaxation of the non-photochemical chlorophyll fluorescence quenching in diatoms: kinetics, components and mechanisms, *Philosophical Transactions of the Royal Society B: Biological Sciences*, 369 (2014) 20130241.
- [22] U.K. Laemmli, Cleavage of structural proteins during the assembly of the head of bacteriophage T4, *Nature*, 227 (1970) 680-685.
- [23] M. Kobayashi, T. Kakizono, N. Nishio, S. Nagai, Effects of light intensity, light quality, and illumination cycle on astaxanthin formation in a green alga, *Haematococcus pluvialis* *Journal-of-Fermentation-and-Bioengineering*, 74 (1992) 61-63.
- [24] M.C. Garcia-Malea, C. Brindley, E. Del Rio, F.G. Acien, J.M. Fernandez, E. Molina, Modelling of growth and accumulation of carotenoids in *Haematococcus pluvialis* as a function of irradiance and nutrients supply, *Biochemical Engineering Journal*, 26 (2005) 107-114.

- [25] B.H.J. Yap, S.A. Crawford, R.R. Dagastine, P.J. Scales, G.J.O. Martin, Nitrogen deprivation of microalgae: effect on cell size, cell wall thickness, cell strength, and resistance to mechanical disruption, *Journal of Industrial Microbiology & Biotechnology*, 43 (2016) 1671-1680.
- [26] P.R. Postma, G. Pataro, M. Capitoli, M.J. Barbosa, R.H. Wijffels, M.H. Eppink, G. Olivieri, G. Ferrari, Selective extraction of intracellular components from the microalga *Chlorella vulgaris* by combined pulsed electric field-temperature treatment, *Bioresource Technology*, 203 (2016) 80-88.
- [27] R.H. Wijffels, M.J. Barbosa, An outlook on microalgal biofuels, *Science*, 329 (2010) 796-799.
- [28] J. Li, D. Zhu, J. Niu, S. Shen, G. Wang, An economic assessment of astaxanthin production by large scale cultivation of *Haematococcus pluvialis*, *Biotechnology Advances*, 29 (2011) 568-574.
- [29] M. Olaizola, M.E. Huntley, Photobioreactor technology and process control: unleashing the industrial potential of microalgal carotenoid pigments, *Book of Abstracts of the 4th International Symposium on natural Colorants for Food, Nutraceuticals, Beverages, Confectionary & Cosmetics*, (2000) 16.
- [30] Y. Cao, E. Ma, S. Cestellos-Blanco, B. Zhang, R. Qiu, Y. Su, J.A. Doudna, P. Yang, Nontoxic nanopore electroporation for effective intracellular delivery of biological macromolecules, *Proceedings of the National Academy of Sciences*, 116 (2019) 7899-7904.
- [31] J. Sheng, R. Vannela, B.E. Rittmann, Evaluation of cell-disruption effects of pulsed-electric-field treatment of *Synechocystis* PCC 6803, *Environmental Science & Technology*, 45 (2011) 3795-3802.
- [32] S. Kroschwald, S. Alberti, Gel or die: phase separation as a survival strategy, *Cell*, 168 (2017) 947-948.
- [33] A.T. Esser, K.C. Smith, T.R. Gowrishankar, Z. Vasilkoski, J.C. Weaver, Mechanisms for the intracellular manipulation of organelles by conventional electroporation, *Biophysical Journal*, 98 (2010) 2506-2514.
- [34] D. Rego, L.M. Redondo, V. Geraldes, L. Costa, J. Navalho, M.T. Pereira, Control of predators in industrial scale microalgae cultures with Pulsed Electric Fields, *Bioelectrochemistry*, 103 (2015) 60-64.
- [35] S.K. Dutcher, E.T. O'Toole, The basal bodies of *Chlamydomonas reinhardtii*, *Cilia*, 5 (2016) 18.
- [36] M. Yamada, G. Goshima, Mitotic spindle assembly in land plants: Molecules and mechanisms, *Biology*, 6 (2017) 6.
- [37] G.J. Pazour, N. Agrin, J. Leszyk, G.B. Witman, Proteomic analysis of a eukaryotic cilium, *The Journal of Cell Biology*, 170 (2005) 103-113.
- [38] L. Wang, L. Gu, D. Meng, Q. Wu, H. Deng, J. Pan, Comparative proteomics reveals timely transport into cilia of regulators or effectors as a mechanism underlying ciliary disassembly, *Journal of Proteome Research*, 16 (2017) 2410-2418.
- [39] H.S. Feiler, T. Desprez, V. Santoni, J. Kronenberger, M. Caboche, J. Traas, The higher plant *Arabidopsis thaliana* encodes a functional CDC48 homologue which is highly expressed in dividing and expanding cells, *The EMBO Journal*, 14 (1995) 5626-5637.
- [40] I.M. Rienties, J. Vink, J.W. Borst, E. Russinova, S.C. de Vries, The *Arabidopsis* SERK1 protein interacts with the AAA-ATPase AtCDC48, the 14-3-3 protein GF14 lambda and the PP2C phosphatase KAPP, *Planta*, 221 (2005) 394-405.
- [41] T.M. Bricker, L.K. Frankel, The structure and function of CP47 and CP43 in Photosystem II, *Photosynthesis Research*, 72 (2002) 131-146.
- [42] A.V. Pigolev, V.V. Klimov, The green alga *Chlamydomonas reinhardtii* as a tool for *in vivo* study of site-directed mutations in PsbO protein of photosystem II, *Biochemistry Moscow*, 80 (2015) 662-673.


- [43] M.M. Najafpour, M.A. Isaloo, J.J. Eaton-Rye, T. Tomo, H. Nishihara, K. Satoh, R. Carpentier, J.-R. Shen, S.I. Allakhverdiev, Water exchange in manganese-based water-oxidizing catalysts in photosynthetic systems: From the water-oxidizing complex in photosystem II to nano-sized manganese oxides, *Biochimica et Biophysica Acta*, 1837 (2014) 1395-1410.
- [44] N.H. Chua, P. Bennoun, Thylakoid membrane polypeptides of *Chlamydomonas reinhardtii*: wild-type and mutant strains deficient in photosystem II reaction center, *Proceedings of the National Academy of Sciences of the United States of America*, 72 (1975) 2175-2179.
- [45] S.P. Mayfield, P. Bennoun, J.D. Rochaix, Expression of the nuclear encoded OEE1 protein is required for oxygen evolution and stability of photosystem II particles in *Chlamydomonas reinhardtii*, *The EMBO Journal*, 6 (1987) 313-318.
- [46] R. Straessner, C. Eing, M. Goettel, C. Gusbeth, W. Frey, Monitoring of pulsed electric field-induced abiotic stress on microalgae by chlorophyll fluorescence diagnostic, *IEEE Transactions on Plasma Science*, 41 (2013) 2951-2958.
- [47] S. Knight, I. Andersson, C.-I. Brändén, Crystallographic analysis of ribulose 1,5-bisphosphate carboxylase from spinach at 2.4 Å resolution: Subunit interactions and active site, *Journal of Molecular Biology*, 215 (1990) 113-160.
- [48] E. Morita, H. Kuroiwa, T. Kuroiwa, H. Nozaki, High localization of ribulose-1,5-bisphosphate carboxylase/oxygenase in the pyrenoids of *Chlamydomonas reinhardtii* (Chlorophyta), as revealed by cryofixation and immunogold electron microscopy, *Journal of Phycology*, 33 (1997) 68-72.
- [49] P.R. Postma, T.L. Miron, G. Olivieri, M.J. Barbosa, R.H. Wijffels, M.H.M. Eppink, Mild disintegration of the green microalgae *Chlorella vulgaris* using bead milling, *Bioresource Technology*, 184 (2015) 297-304.
- [50] L. Recuenco-Muñoz, P. Offre, L. Valledor, D. Lyon, W. Weckwerth, S. Wienkoop, Targeted quantitative analysis of a diurnal RuBisCO subunit expression and translation profile in *Chlamydomonas reinhardtii* introducing a novel Mass Western approach, *Journal of Proteomics*, 113 (2015) 143-153.
- [51] R. Trosch, T. Muhlhaus, M. Schroda, F. Willmund, ATP-dependent molecular chaperones in plastids - More complex than expected, *Biochimica et Biophysica Acta - Bioenergetics*, 1847 (2018) 872-888.
- [52] Y.Z. Zhang, H. Launay, F. Liu, R. Lebrun, B. Gontero, Interaction between adenylate kinase 3 and glyceraldehyde-3-phosphate dehydrogenase from *Chlamydomonas reinhardtii*, *FEBS Journal*, 285 (2018) 2495-2503.
- [53] K. Asada, M.R. Badger, Photoreduction of $^{18}\text{O}_2$ and $\text{H}_2^{18}\text{O}_2$ with concomitant evolution of $^{16}\text{O}_2$ in intact spinach chloroplasts: evidence for scavenging of hydrogen peroxide by peroxidase, *Plant and Cell Physiology*, 25 (1984) 1169-1179.
- [54] K. Asada, THE water-water cycle in chloroplasts: scavenging of active oxygens and dissipation of excess photons, *Annual Review of Plant Physiology and Plant Molecular Biology*, 50 (1999) 601-639.
- [55] M. Yusupov, J. Van der Paal, E.C. Neyts, A. Bogaerts, Synergistic effect of electric field and lipid oxidation on the permeability of cell membranes, *Biochimica et Biophysica Acta - General Subjects*, 1861 (2017) 839-847.
- [56] S. Takahashi, N. Murata, Interruption of the Calvin cycle inhibits the repair of photosystem II from photodamage, *Biochimica et Biophysica Acta - Bioenergetics*, 1708 (2005) 352-361.
- [57] O. Sayanova, V. Mimouni, L. Ulmann, A. Morant-Manceau, V. Pasquet, B. Schoefs, J.A. Napier, Modulation of lipid biosynthesis by stress in diatoms, *Philosophical Transactions of the Royal Society B: Biological Sciences*, 372 (2017) 1728.
- [58] A. Lei, H. Chen, G. Shen, Z. Hu, L. Chen, J. Wang, Expression of fatty acid synthesis genes and fatty acid accumulation in *Haematococcus pluvialis* under different stressors, *Biotechnology for Biofuels*, 5 (2012) 18.

- [59] J.S. Sussenbach, P.J. Strijkert, Arginine metabolism in *Chlamydomonas reinhardtii*. A new type of citrulline degradation, *FEBS Letters*, 7 (1970) 274-276.
- [60] G.A. Elhag, F.J. Thomas, T.P. McCreery, D.P. Bourque, Nuclear-encoded chloroplast ribosomal protein L12 of *Nicotiana tabacum*: characterization of mature protein and isolation and sequence analysis of cDNA clones encoding its cytoplasmic precursor, *Nucleic Acids Research*, 20 (1992) 689-697.
- [61] M.J. Brauer, C. Huttenhower, E.M. Airoidi, R. Rosenstein, J.C. Matese, D. Gresham, V.M. Boer, O.G. Troyanskaya, D. Botstein, Coordination of growth rate, cell cycle, stress response, and metabolic activity in yeast, *Molecular Biology of the Cell*, 19 (2008) 352-367.
- [62] N.-H. Chua, G. Blobel, P. Siekevitz, G.E. Palade, Attachment of Chloroplast Polysomes to Thylakoid Membranes in *Chlamydomonas reinhardtii*, *Proceedings of the National Academy of Sciences*, 70 (1973) 1554-1558.
- [63] S.L. Baldauf, J.R. Manhart, J.D. Palmer, Different fates of the chloroplast *tufA* gene following its transfer to the nucleus in green algae, *Proceedings of the National Academy of Sciences of the United States of America*, 87 (1990) 5317-5321.
- [64] B.S. Negrutskii, A.V. El'skaya, Eukaryotic translation elongation factor 1 α : structure, expression, functions, and possible role in aminoacyl-tRNA channeling, in: K. Moldave (Ed.) *Progress in Nucleic Acid Research and Molecular Biology*, Academic Press 1998, pp. 47-78.
- [65] R.C. Thompson, *Trends in Biochemical Sciences*, 13 (1980) 91-93.
- [66] G.L. Kogan, V.A. Gvozdev, Multifunctional nascent polypeptide-associated complex (NAC), *Molecular Biology*, 48 (2014) 189-196.
- [67] B. Cevher-Keskin, ARF1 and SAR1 GTPases in endomembrane trafficking in plants, *International Journal of Molecular Sciences*, 14 (2013) 18181-18199.
- [68] D. Dutta, J.G. Donaldson, Rab and Arf G proteins in endosomal trafficking, in: W. Guo (Ed.) *Methods in Cell Biology*, Academic Press 2015, pp. 127-138.
- [69] H. Heide, A. Nordhues, F. Drepper, S. Nick, M. Schulz-Raffelt, W. Haehnel, M. Schroda, Application of quantitative immunoprecipitation combined with knockdown and cross-linking to *Chlamydomonas* reveals the presence of vesicle-inducing protein in plastids 1 in a common complex with chloroplast HSP90C, *Proteomics*, 9 (2009) 3079-3089.
- [70] P. Guo, S. Jiang, C. Bai, W. Zhang, Q. Zhao, C. Liu, Asymmetric functional interaction between chaperonin and its plastidic cofactors, *FEBS Journal*, 282 (2015) 3959-3970.
- [71] J. Shanklin, N.D. DeWitt, J.M. Flanagan, The stroma of higher plant plastids contain ClpP and ClpC, functional homologs of *Escherichia coli* ClpP and ClpA: an archetypal two-component ATP-dependent protease, *The Plant Cell*, 7 (1995) 1713-1722.
- [72] G.D. Markham, M.A. Pajares, Structure-function relationships in methionine adenosyltransferases, *Cellular and Molecular Life Sciences*, 66 (2009) 636-648.
- [73] F. Thiebaut, A.S. Hemerly, P.C.G. Ferreira, A role for epigenetic regulation in the adaptation and stress responses of non-model plants, *Frontiers in Plant Science*, 10 (2019).
- [74] J. de la Cruz, D. Kressler, P. Linder, Unwinding RNA in *Saccharomyces cerevisiae*: DEAD-box proteins and related families, *Trends in Biochemical Sciences*, 24 (1999) 192-198.
- [75] Y. Lemoine, B. Schoefs, Secondary ketocarotenoid astaxanthin biosynthesis in algae: a multifunctional response to stress, *Photosynthesis Research*, 106 (2010) 155-177.
- [76] F. Bai, C. Gusbeth, W. Frey, P. Nick, Nanosecond pulsed electric fields trigger cell differentiation in *Chlamydomonas reinhardtii*, *Biochimica et Biophysica Acta*, 1859 (2017) 651-661.
- [77] J. Voigt, I. Liebich, M. Kieß, R. Frank, Subcellular distribution of 14-3-3 proteins in the unicellular green alga *Chlamydomonas reinhardtii*, *European Journal of Biochemistry*, 268 (2001) 6449-6457.

- [78] T. Mukherjee, J. Hanes, I. Tews, S.E. Ealick, T.P. Begley, Pyridoxal phosphate: Biosynthesis and catabolism, *Biochimica et Biophysica Acta (BBA) - Proteins and Proteomics*, 1814 (2011) 1585-1596.
- [79] K.C. Smith, R.S. Son, T.R. Gowrishankar, J.C. Weaver, Emergence of a large pore subpopulation during electroporating pulses, *Bioelectrochemistry*, 100 (2014) 3-10.
- [80] J. Marchand, P. Heydarizadeh, B. Schoefs, C. Spetea, Ion and metabolite transport in the chloroplast of algae: lessons from land plants, *Cellular and Molecular Life Sciences*, 75 (2018) 2153-2176.
- [81] F. Chemat, M.A. Vian, G. Cravotto, Green extraction of natural products: concept and principles, *International Journal of Molecular Sciences*, 13 (2012) 8615-8627.
- [82] J.R. Mielenz, Biofuels from protein, *Nature Biotechnology*, 29 (2011) 327-328.
- [83] Y.-X. Huo, K.M. Cho, J.G.L. Rivera, E. Monte, C.R. Shen, Y. Yan, J.C. Liao, Conversion of proteins into biofuels by engineering nitrogen flux, *Nature Biotechnology*, 29 (2011) 346-351.

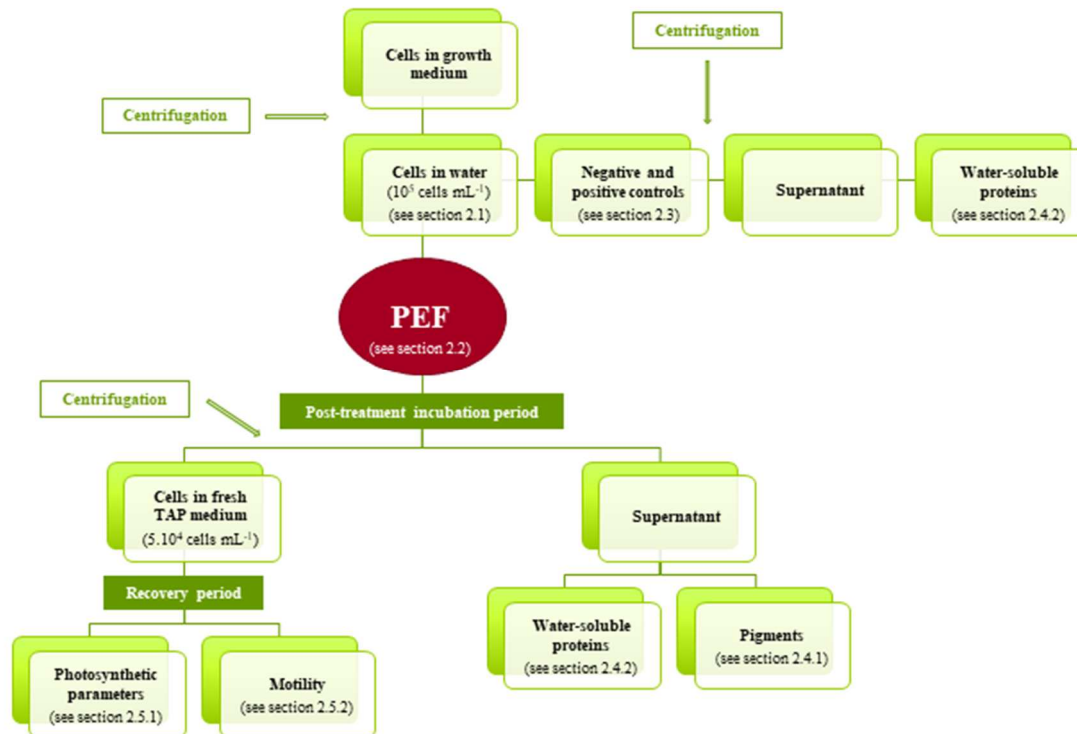
Vitae

	<p>Vincent BLANCKAERT, born in 1961, associate professor in cell biology since September 1993 at the IUT of Laval, Le Mans University, France. He is attached to the team EA-2160 (MMS): —Sea, Molecules, Health. From 1991 to 1993, he was a postdoctoral fellow at the Department of Genetics and Cell Biology, Washington State University, Pullman, WA, USA after his PhD obtained in 1990 in the field of "Life and Health Sciences" at University of Lille 1. His research topics are focusing on molecules and cancer, protein purification, use of pulsed electric field or corona discharges in bacterial decontamination and in molecule-derived microalgae electroextraction.</p>
	<p>Brigitte VEIDL - Assistant engineer in biology since 5 years at Le Mans University. My skills are microalgae culture to study their responses to stress. Implementation of analytical and physiological methods.</p>
	<p>Justine MARCHAND - Molecular biologist, I graduated at the U. of Brest (France) and became an assistant professor in the 'Mer Molécules Santé' laboratory at Le Mans U. in the 'Metabolism, Microalgal engineering, Molecules and Applications' (MIMMA) team. My research is orientated toward transcriptomic and bioengineering studies in microalgae and aim at understanding the regulatory mechanisms leading to modifications of the management of carbon atoms under stress conditions in marine microalgae and especially the diatom <i>Phaeodactylum tricornutum</i>. A special attention is paid to identify the role of transcription factors in the regulation and reorientation of carbon metabolism in order to control carbon fluxes toward compounds of interest (lipids, carotenoids). I am also working on the development of innovative methods for extracting molecules from microalgae such as the use of pulse electric fields</p>

 A portrait of Benoît Schoefs, a middle-aged man with grey hair and a mustache, wearing a light-colored sweater. He is standing outdoors with greenery in the background.	<p>Benoît SCHOEFS - Plant physiologist, I graduated from the Liège U, Belgium. I became Professor in Plant Physiology at the Dijon U. In 2011, I joined Le Mans U. where I lead a team working on stress management and carbon metabolism in microalgae. My research focuses on basic and applied aspects of the physiological, biochemical and molecular responses of photosynthetic organisms to stresses. I have published 90 papers. I am a member of the editorial board of Frontiers in Plant Science, Marine Drugs and Botany Letters. I have been laureate of the Prize 'D. Clos' and the annual scientific competition of the Belgian Academy of Science.</p>
--	---

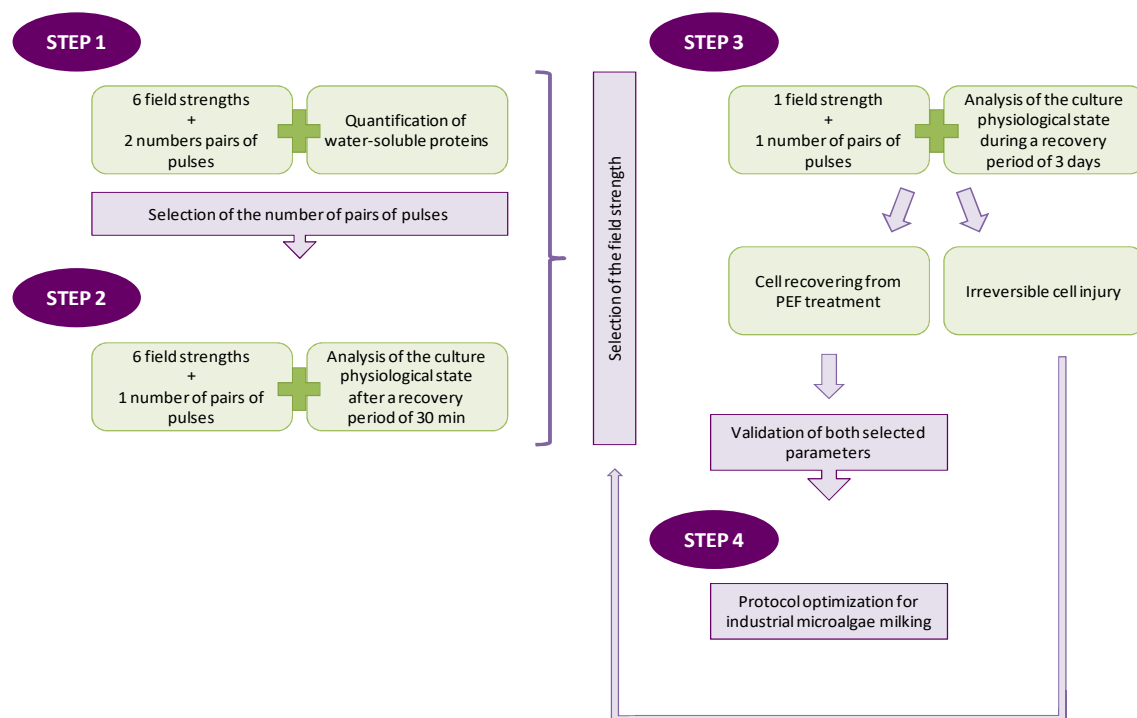
To be reproduced in color

Schematic 1. Overview of the standard protocol applied to the microalgae from their harvesting until the analysis of their physiological status following the PEF treatment.



To be reproduced in color

Schematic 2. Schematic representation of the global experimental approach.



To be reproduced in color

Schematic 3. Overview of the PEF-treatment protocol optimisation tests. Protocol 5 corresponds to the protocol applied in the previous experiments. In the four other protocols, the recovery period was deleted (protocols 1 and 4), the duration of the incubation period was reduced (protocols 1 to 3), and/or cells were transferred in fresh distilled water instead of TAP medium at the end of the incubation period (protocol 2). Centrifugations a1 and a2 were performed at the end of the incubation period while centrifugations b1, b2 and b3 were performed at the end of the recovery period.

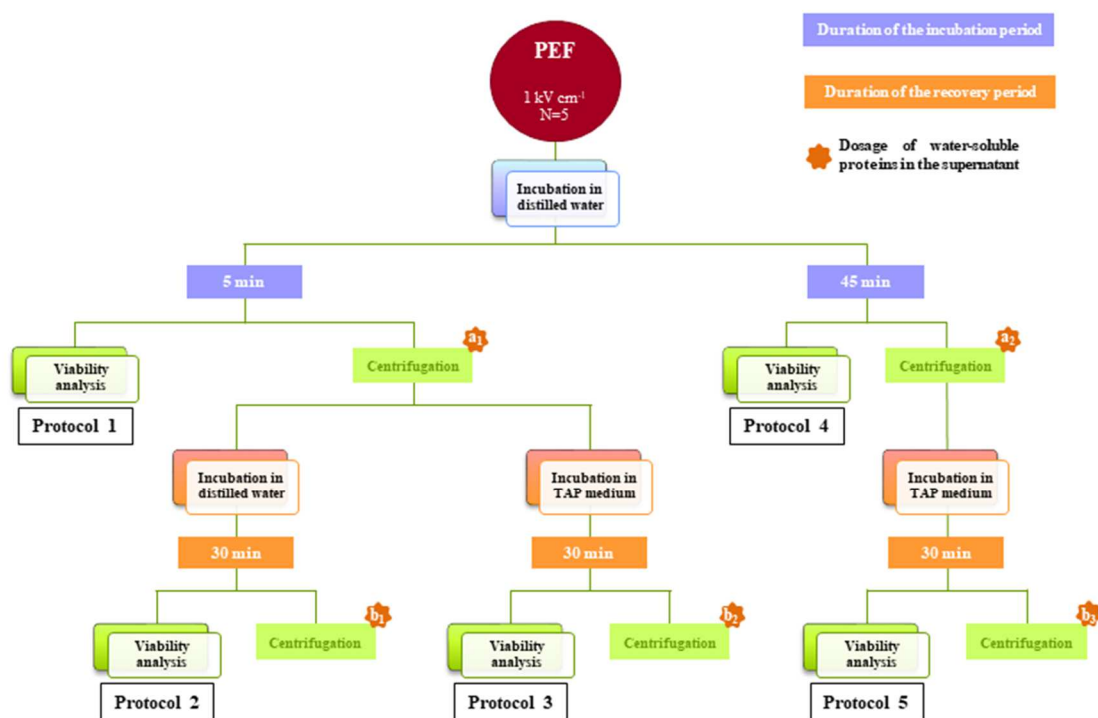


Figure 1. Evolution of the cell density of *Haematococcus pluvialis* cultures for the tested carbon sources (MLA: NaHCO_3 (○), BG11: Na_2CO_3 (△), TAP: acetate (◇, ◆)) and illumination conditions (open symbols: photon flux density of $35 \mu\text{mol photons m}^{-2} \text{s}^{-1}$ with a photoperiod of 14 h, close symbols: darkness).



Figure 2. Influence of the field strength and the number of pulses on the release of water-soluble proteins from PEF-treated microalgae. Six field strengths (from 0 to 6 kV cm⁻¹) and two numbers of pulses (N=5 or 9) were applied to the microalgae suspended in water (10⁵ cells mL⁻¹). Measurements of protein concentrations were performed 45 min after the end of the PEF treatment, using the supernatants obtained after centrifugation of the treated microalgae suspensions. Negative and positive controls were performed according to the protocol described in section 2.3. * indicates values that are significantly different from the control condition (0 kV cm⁻¹) (*p* value < 0.05).

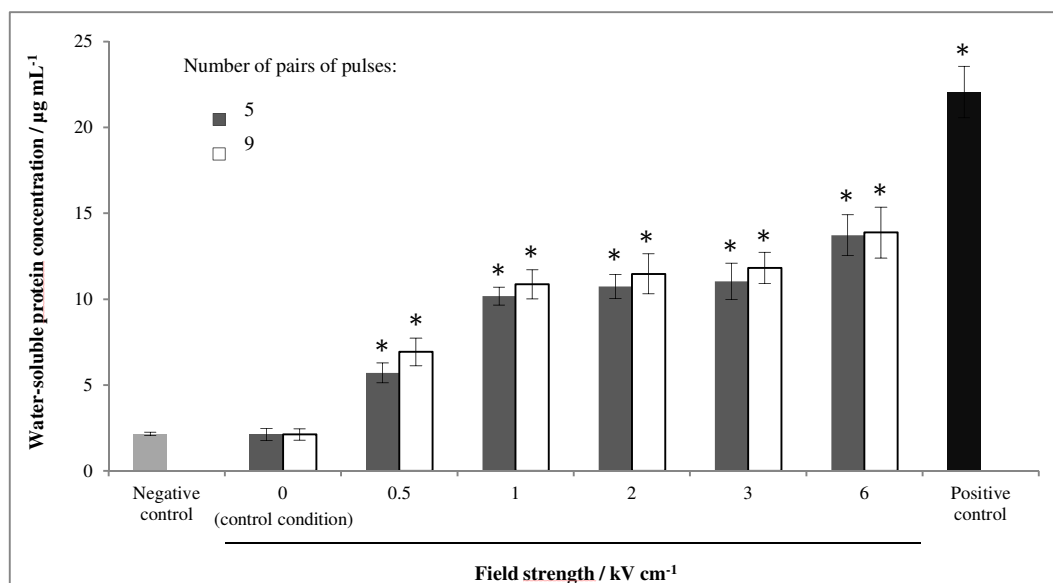


Figure 3. Influence of the PEF strength on the physiological state of a cell culture of *H. pluvialis*. Cells were exposed to field strengths from 0 to 6 kV cm⁻¹. The number of pairs of pulses was set to 5. Four physiological parameters were studied: (A) percentage of motile cells, (B) gross photosynthesis rate, (C) Fv/Fm ratio (r.u.: relative units), and (D) respiration rate. Measurements were performed 30 min after cells were returned to the growth conditions (TAP medium; 35 μ moles of photons m⁻² s⁻¹). * indicates values that are significantly different from the control condition (0 kV cm⁻¹) (p value < 0.05).

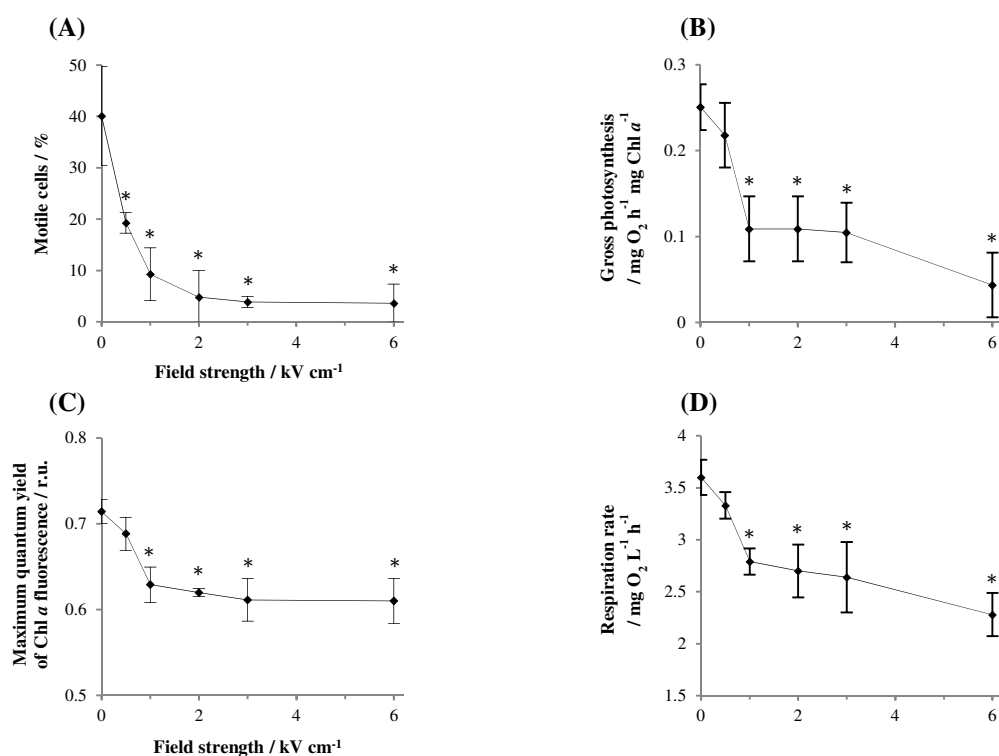


Figure 4. Impact of applied PEF field strength on cell permeability.

(A) Cell permeability was estimated by microscopically assessing the proportion of cells that had internalized the Evans blue dye.

(B) Effects of the electric field strength on the relative abundance of the different cell populations (RP_p (◆), IP_p (▲), N-PEF_p (●) and NA_{pp} (■) cells)

(C) Variation of the BI index in function of the applied field strength

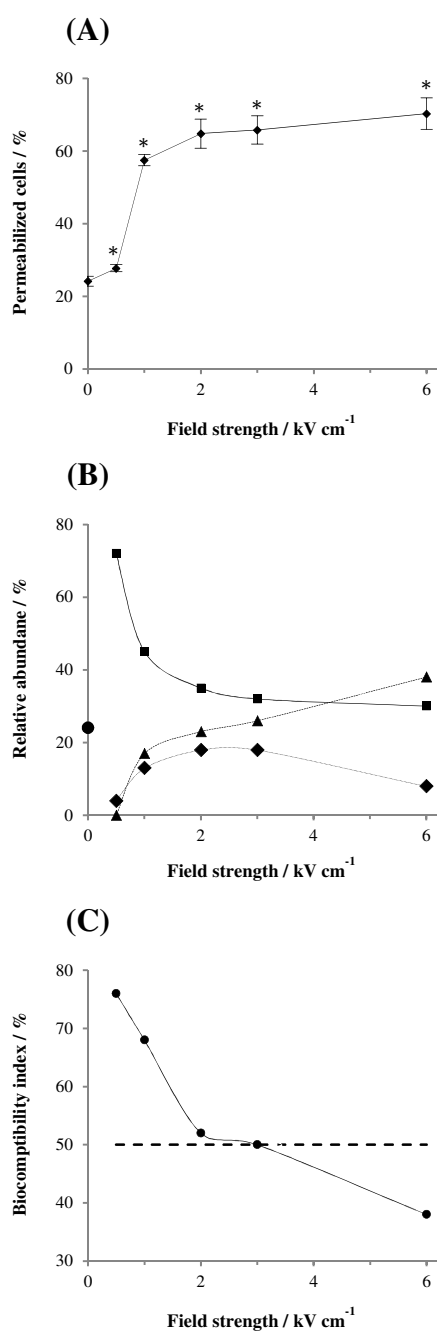


Figure 5. Monitoring of the physiological state of cultures after they were exposed to a field strength of 1 kV cm^{-1} . The number of pairs of pulses was set at 5. Four physiological parameters were followed: (A) percentage of motile cells, (B) cell density, (C) gross photosynthesis rate and (D) Fv/Fm ratio (r.u.: relative units). Measurements were every 24 h during a period of three days which started about 30 min after the cells were returned to the original growth condition (TAP medium; $35 \mu\text{moles of photons m}^{-2} \text{ s}^{-1}$). The dotted line corresponds to the field strength studied (1 kV cm^{-1}) and the solid line to the control condition (0 kV cm^{-1}). * indicates values that are significantly different from the control condition (0 kV cm^{-1}) (p value < 0.05).

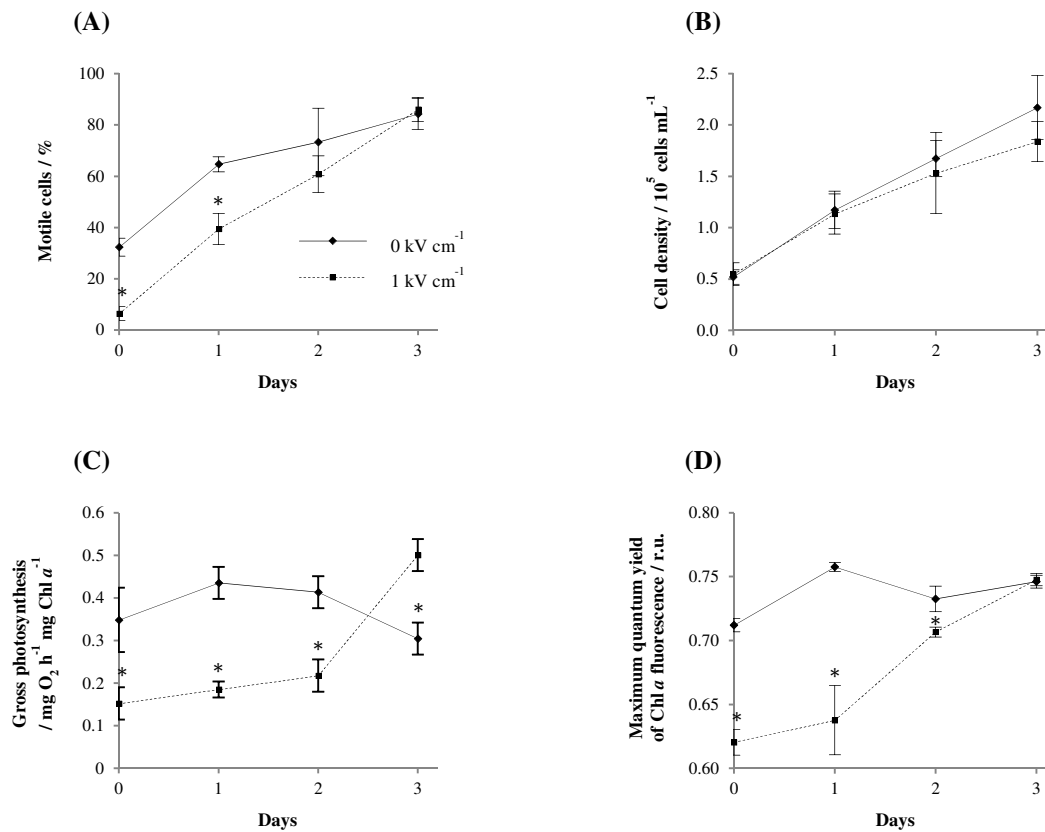
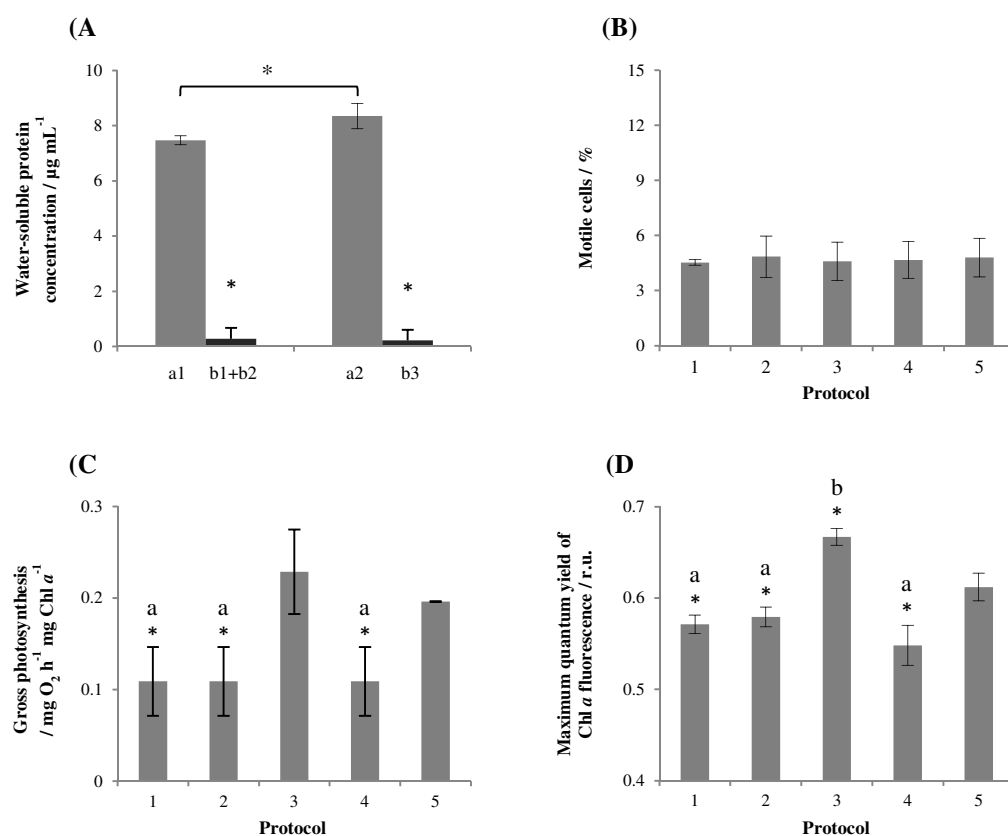


Figure 6. (A) Protein release from PEF-treated cells during the incubation (a1 and a2) or the recovery period (b1+b2 and b3), and physiological state of cultures treated according to one of the five protocols described in Schematic 3. Three physiological parameters were studied: (B) percentage of motile cells, (C) gross photosynthesis rate, and (D) Fv/Fm ratio (r.u.: relative units). The field strength was set at 1 kV cm^{-1} and the number of pairs of pulses at 5. * indicates values that are significantly different from that obtained with protocol 5 (p value < 0.05).



Supplemental data 1-2

Supplemental data 1 presents the morphologic characters and the taxonomic positioning of the new strain

Supplemental data 2 presents the distribution of the F  ret cell diameters within the population of *Haematococcus pluvialis* used in the biocompatible electroextraction of proteins.

Supplemental data 3

Supplemental data 3, presented as a Excel document in additional data with the sheet titled “electroextraction synthesis” showed that peptide matches reflect empirically the amount of electro-extracted proteins from both 0.5 and 1 kV cm⁻¹ conditions. Each protein was presented in the table with their characteristics and their biological functions as found in databases. The proteins with cells in grey are the one that were present in both PEF conditions 0.5 and 1 kV cm⁻¹. It can be noticed that the quantity in peptides is ever more important with the condition to 1 kV cm⁻¹. These data also show that the increase in the number of electro-extracted proteins is field-dependent; increasing electric-field being able to electro-permeation of organelles with a lower size. This has also being reported in *Chlorella vulgaris* (Postma et al., 2016). Thus with PEF 0.5 kV cm⁻¹ the main proteins extracted provided from cytoplasm and chloroplast while at 1 kVcm⁻¹ a larger number of protein were extracted from chloroplast, mitochondrion, nucleus and cytoplasm.

Supplemental data 4

Supplemental data 4 presents the spectral characterization of the pigments electro-extracted from *Haematococcus pluvialis*.

Table 1. List of the identified proteins

Protein #	Accession Description
1	A0A097KLQ1 gi 698348597 gb AIT94116.1 CP43 chlorophyll apoprotein of photosystem II
2	A0A0S2IDE6 A0A0S2IDE6_HAEPL ATP synthase subunit alpha
3	A0A0S2IDH6 A0A0S2IDH6_HAEPL ATP synthase subunit beta
4	F8WLT0 F8WLT0_9CHLO ATP synthase subunit beta
5	Q8HDD9 Q8HDD9_9CHLO ATP synthase subunit beta
6	A0A0U4MVM8 A0A0U4MVM8_9CHLO ATP synthase
7	A8J0E4_CHLRE gi 158276511 gb EDP02283.1 oxygen-evolving enhancer protein 1 of photosystem II
8	A0A0H5BIH2 A0A0H5BIH2_9CHLO Ribulose biphosphate carboxylase large chain
9	A0A0S2IDA4 A0A0S2IDA4_HAEPL Ribulose biphosphate carboxylase large chain
10	A1E8X4_9CHLO Ribulose biphosphate carboxylase large chain (Fragment)
11	D2YZF3 D2YZF3_9CHLO Ribulose biphosphate carboxylase large chain (Fragment)
12	O98765 O98765_9CHLO Ribulose biphosphate carboxylase large chain
13	tr A0A0S2ICK1 A0A0S2ICK1_9CHLO Ribulose biphosphate carboxylase large chain
14	A8IYP4 A8IYP4_CHLRE Phosphoribulokinase
15	B1PL92 B1PL92_DUNSA Glyceraldehyde-3-phosphate dehydrogenase
16	D8U9J4 D8U9J4_VOLCA Glyceraldehyde-3-phosphate dehydrogenase
17	A0A0S1VVL8 A0A0S1VVL8_9CHLO DEAD box RNA helicase CιRH4 (Fragment)
18	A8JBX6 A8JBX6_CHLRE Nascent polypeptide-associated complex subunit beta
19	A8HX38 A8HX38_CHLRE Eukaryotic translation elongation factor 1 alpha 1
20	P51821 ARF1_CHLRE ADP-ribosylation factor 1
21	D8TT41 D8TT41_VOLCA Luminal binding protein Bip1
22	Q94IK4 Q94IK4_SCHDU Luminal binding protein, BiP
23	A0A0S2IDP1 A0A0S2IDP1_HAEPL 30S ribosomal protein S2, chloroplastic
24	A8HTY0 A8HTY0_CHLRE Plastid ribosomal protein L7/L12
25	A0A0S2IEF9 A0A0S2IEF9_HAEPL Elongation factor Tu, chloroplastic
26	A0A0S2LNT6 A0A0S2LNT6_9CHLO Elongation factor Tu, chloroplastic
27	A0A0S2ICY2 A0A0S2ICY2_HAEPL 30S ribosomal protein S3, chloroplastic
28	D9CIY7 D9CIY7_VOLCA S-adenosylmethionine synthase
29	A8HYU5 METK_CHLRES S-adenosylmethionine synthase
30	G9B655 G9B655_HAEPL Acyl carrier protein
31	D8TV86 D8TV86_VOLCA Argininosuccinate synthase
32	E5G3Q8 E5G3Q8_9CHLO Beta-tubulin (Fragment)
33	O22660 O22660_9CHLO Tubulin alpha chain
34	QJJ4J6 Q4JJ6_DUNSA Tubulin beta chain (Fragment)

35	A8IXZ0 A8IXZ0_CHLRE Tubulin beta chain
36	A8HW56 A8HW56_CHLRE Flagellar associated protein
37	H2DQ69 H2DQ69_HAEPL Heat shock protein 70
38	A8HYV3 A8HYV3_CHLRE Heat shock protein 70B
39	Q3I5Q5 Q3I5Q5_VOLCA Heat-shock inducible Hsp70
40	Q8VY41 Q8VY41_DUNSA Heat shock protein 70B
41	Q3L2Z3 Q3L2Z3_HAEPL Superoxide dismutase
42	Q1WLZ5 Q1WLZ5_CHLIN 14-3-3-like protein-related protein
43	Q52R84 Q52R84_HAEPL 14-3-3 protein
44	Q56D00 Q56D00_DUNSA 14-3-3 protein
45	A8ITH8 A8ITH8_CHLRE Chaperonin 60B2
46	D8U1H9 D8U1H9_VOLCA Putative uncharacterized protein
47	A8JDV2 A8JDV2_CHLRE Predicted protein (Fragment)
48	D8U1R3 D8U1R3_VOLCA Putative uncharacterized protein
49	D8TLB0 D8TLB0_VOLCA Putative uncharacterized protein
50	D8TZZ8 D8TZZ8_VOLCA Putative uncharacterized protein
51	D8TII3 D8TII3_VOLCA Putative uncharacterized protein
52	D8TY33 D8TY33_VOLCA Putative uncharacterized protein

Table 2. Summary of the functional categories assigned to the electro-extracted proteins from *H. pluvialis*.

1. Core metabolism, 29 proteins, 55% <ul style="list-style-type: none"> - Energy production - Protein biosynthesis - Lipid biosynthesis - Signalling 	2. Stress response, 9 proteins, 17% <ul style="list-style-type: none"> - Nucleic acids - Oxidative stress
3. Cell movement, 7 proteins, 14% <ul style="list-style-type: none"> - Flagella - Cytoskeleton - Trafficking 	4. Unassigned proteins, 7 proteins, 14%

Table 3. The variations of the different cell populations obtained with each PEF intensity. BI: biocompatible index, NA_p: nonaffected cells, IP_p and RP_p: irreversibly and reversibly permeabilized cells, respectively, NAT-P_p and N-PEF_p: naturally permeabilized celles without and with peristaltic pump, respectively.

Field intensity (kV cm ⁻¹)	Relative abundance (%)							
	NAT-P _p	N-PEF _p – 5 min	N-PEF _p – 45 min	NA _{pp}	IP _p +RP _p	RP _p	IP _p	BI
0	8	24	24	0	0	0	0	-
0.5	-	-		72	4	4	0	76
1	-	-		45	31	13	17	68
2	-	-		34	41	18	23	52
3	-	-		32	44	18	26	50
6	-	-		30	46	8	38	38

Table 4. Calculated energy input corresponding to each PEF field intensity and number of pulses tested. The values indicated in bold and italic characters indicate the energy input producing the highest proportion of RP cells and a BI under 50%, respectively.

	$W_{\text{PEF}} (\text{kJ m}^{-3})$		$W_{\text{PEF}} (\text{kJ kg}^{-1})$	
$E_{\text{PEF}} (\text{kV cm}^{-1})$	$N_{\text{pulse}} = 5$	$N_{\text{pulse}} = 9$	$N_{\text{pulse}} = 5$	$N_{\text{pulse}} = 9$
0.0	0.00E+00	0.00E+00	0.00	0.00
0.5	5.00E+01	9.00E+01	0.05	0.09
1.0	2.00E+02	3.60E+02	0.20	0.36
2.0	8.00E+02	1.44E+03	0.80	1.44
3.0	<i>1.80E+03</i>	3.24E+03	<i>1.80</i>	3.24
4.0	3.20E+03	5.76E+03	3.20	5.77
5.0	5.00E+03	9.00E+03	5.01	9.01
6.0	7.20E+03	1.30E+04	7.21	12.97